frontiers in Plant Science

ORIGINAL RESEARCH
published: 22 May 2019
doi: 10.3389/fpls.2019.00635

Manipulating Endoplasmic Reticulum-Plasma Membrane Tethering in Plants Through Fluorescent Protein Complementation

Kai Tao[1,2], *Justin R. Waletich*[2], *Felipe Arredondo*[2] *and Brett M. Tyler*[1,2,3]*

[1] Molecular and Cellular Biology Program, Oregon State University, Corvallis, OR, United States, [2] Department of Botany and Plant Pathology, Oregon State University, Corvallis, OR, United States, [3] Center for Genome Research and Biocomputing, Oregon State University, Corvallis, OR, United States

OPEN ACCESS

Edited by:
Diane C. Bassham,
Iowa State University, United States

Reviewed by:
Abel Rosado,
University of British Columbia, Canada
Lorenzo Frigerio,
University of Warwick, United Kingdom
Xiaohong Zhuang,
The Chinese University of Hong Kong, China

***Correspondence:**
Brett M. Tyler
brett.tyler@oregonstate.edu

Specialty section:
This article was submitted to Plant Cell Biology, a section of the journal Frontiers in Plant Science

Received: *15 January 2019*
Accepted: *26 April 2019*
Published: *22 May 2019*

Citation:
Tao K, Waletich JR, Arredondo F and Tyler BM (2019) Manipulating Endoplasmic Reticulum-Plasma Membrane Tethering in Plants Through Fluorescent Protein Complementation. Front. Plant Sci. 10:635. doi: 10.3389/fpls.2019.00635

The bimolecular fluorescence complementation (BiFC) assay has been widely used to examine interactions between integral and peripheral proteins within putative plasma membrane (PM) microdomains. In the course of using BiFC assays to examine the co-localization of plasma membrane (PM) targeted receptor-like kinases (RLKs), such as FLS2, with PM micro-domain proteins such as remorins, we unexpectedly observed heterogeneous distribution patterns of fluorescence on the PM of *Nicotiana benthamiana* leaf cortical cells. These patterns appeared to co-localize with the endoplasmic reticulum (ER) and with ER-PM contact sites, and closely resembled patterns caused by over-expression of the ER-PM tether protein Synaptotagmin1 (SYT1). Using domain swap experiments with SYT1, we inferred that non-specific dimerization between FLS2-VenusN and VenusC-StRem1.3 could create artificial ER-PM tether proteins analogous to SYT1. The same patterns of ER-PM tethering were produced when a representative set of integral membrane proteins were partnered in BiFC complexes with PM-targeted peripheral membrane proteins, including PtdIns(4)P-binding proteins. We inferred that spontaneous formation of mature fluorescent proteins caused the BiFC complexes to trap the integral membrane proteins in the ER during delivery to the PM, producing a PM-ER tether. This phenomenon could be a useful tool to deliberately manipulate ER-PM tethering or to test protein membrane localization. However, this study also highlights the risk of using the BiFC assay to study membrane protein interactions in plants, due to the possibility of alterations in cellular structures and membrane organization, or misinterpretation of protein-protein interactions. A number of published studies using this approach may therefore need to be revisited.

Keywords: tethering, plasma membrane, endoplasmic recticulum, peripheral membrane protein, integral membrane protein

SIGNIFICANCE STATEMENT

The bimolecular fluorescence complementation (BiFC) assay has been widely used to examine interactions between integral and peripheral proteins within putative plasma membrane (PM) microdomains. Using domain swap experiments involving the endoplasmic reticulum-PM tether protein SYT1, we have obtained evidence that BiFC complexes involving one integral membrane protein and one peripheral membrane protein can act as synthetic EM-PM tethers, producing images that resemble microdomain co-localization, but are actually artifacts; a number of published studies should thus be revisited.

INTRODUCTION

A variety of internal organelles and structures are closely associated with the PM, especially in plant cells where the large central vacuole compresses the cytoplasm into a thin layer against the PM. These include endosomes, multi-vesicular bodies (MVBs), cortical microtubules, actin filaments, and cortical layers of the endoplasmic reticulum (ER). The ER is the largest membrane-bound organelle comprising an expansive network throughout the cell, functioning in protein synthesis and modification, lipid biosynthesis, metabolism, and Ca^{2+} and other intracellular signaling (Burgoyne et al., 2015). In order to coordinate its specialized functions with other membrane-bound organelles or the PM, the ER is functionally connected through vesicular trafficking, which involves the fusion of the membranes of interacting organelles. As an alternative mechanism of communication, tethering structures known as membrane contact sites (MCSs) provide a transient or durable "bridge" between the ER and other organelles including the PM. MCSs maintain the participating membranes in close proximity without membrane fusion taking place, enabling inter-organelle communication and exchange of metabolites (Helle et al., 2013; Perez-Sancho et al., 2016). MCSs formed by the PM and the ER are called ER-PM contact sites (EPCSs). These sites have been characterized in a variety of eukaryotic species, including animals, yeast, and plants (Saheki and De Camilli, 2017; Wang et al., 2017). EPCSs are precisely maintained and regulated by a variety of protein tethers or protein complexes. Though it has been suggested that each of these tethers or protein groups is associated with different cellular functions, all of them share the same structural characteristics: an ER-anchored region that can be either a hydrophobic hairpin inserted into the ER membrane or a transmembrane domain (TMD) integrated into the ER, combined with a cytosolic domain that contains motifs for binding lipids or proteins in the PM (Prinz, 2014; Saheki and De Camilli, 2017; Wang et al., 2017).

In plants, two different major protein groups sharing these common features have been identified as tethers at EPCSs, namely Synaptogamins (SYTs) and Vesicle-associated membrane protein-Associated Proteins (VAPs). One well-characterized tether protein is *Arabidopsis* Synaptogamin 1 (SYT1, also known as SYTA). SYT1 contains a TMD at the N terminus, a synaptotagmin-like-mitochondria-lipid binding domain (SMP) close to the TMD, and a C-terminal cytoplasmic domain containing two conserved calcium-binding domains C2A and C2B that are responsible for binding a variety of negatively charged phospholipids on the PM (Schapire et al., 2008; Yamazaki et al., 2010; Levy et al., 2015; Pérez-Sancho et al., 2015). The TMD mediates ER-anchoring and the C2AC2B domain mediates PM-binding, together conferring the ER-PM tethering function of SYT1. Plant EPCSs have also been shown to contain VAP27-1 and VAP27-3 which are homologous to mammalian VAPs (Wang et al., 2014, 2016). The C-terminal domains of the VAP27s are examples of integral membrane tail-anchoring domains, and anchor the VAP27s to the ER membrane. PM-binding of the VAP27s is via interaction of their N-terminal conserved major sperm domain (MSD) with the NETWORKED protein, NET3C, as well as cytoskeletal elements. NET3C is plant-specific and located in EPCSs. In addition, VAP27s were also found to form protein complexes with plant oxysterol-binding-protein-related proteins (ORPs), which contain pleckstrin homology (PH) domains for the binding of phosphoinositides (PIPs) in the PM (Saravanan et al., 2009). Furthermore, VAP27 was recently shown to directly interact with clathrin and with PIPs at endocytic subdomains in the PM, resulting in the establishment of tethering (Stefano et al., 2018).

The bimolecular fluorescence complementation (BiFC) assay (Kerppola, 2008) is a commonly used experimental approach to study protein-protein interactions (Kerppola, 2008). The BiFC assay is based on two non-fluorescing fragments split from a fluorescent protein, each of which is translationally fused with a different protein of interest; interaction between the proteins of interest will bring the two non-fluorescing fragments into proximity with each other resulting in the re-assembly of a functional fluorescent protein (Kerppola, 2006). Thus, the BiFC assay not only enables identification of a potential protein-protein interaction, but also allows direct visualization of the protein complex *in vivo*. Due to these useful characteristics, the BiFC assay has also been successfully applied as a high-throughput approach in several large-scale studies to map potential protein-protein interactions (Remy and Michnick, 2004; Boruc et al., 2010; Snider et al., 2013). Venus, a variant of enhanced yellow fluorescence protein (EYFP) with a higher efficiency of maturation and better adaptability in acid and high temperature environments, has become a widely used fluorescent protein for BiFC assays (Saka et al., 2007; Kodama and Hu, 2010; Miller et al., 2015). Moreover, a residue at position 155 has proven useful as a split site for Venus in BiFC assays (Wong and O'Bryan, 2011; Kodama and Hu, 2012). However, a challenge for this strategy is the spontaneous reassembly of the two fragments in the absence of associating protein partners that can result in false positive BiFC signals (Shyu et al., 2006; Zamyatnin et al., 2006; Saka et al., 2007).

Growing evidence has revealed that different phospholipid species and membrane proteins in the PM may be organized into coalescences with diameters ranging from 2.0 to 300 nm, referred to as "lipid or membrane rafts" or more recently as "microdomains" (Kusumi et al., 2011; Lillemeier and Klammt, 2012; Varshney et al., 2016). These microdomains are the result of lipid-lipid, protein-lipid, and protein-protein interactions in the

plasma membrane, potentially providing functional platforms to orchestrate a multitude of signaling pathways (Kusumi et al., 2012). To date, two major protein families, called flotillins and remorins have been associated with plasma membrane microdomains (Raffaele et al., 2009). Flotillins are widely present in all kingdoms of life, and their membrane targeting is mediated by either myristoylation, palmitoylation, or both (Jarsch et al., 2014). In contrast, remorins are plant-specific proteins, which have been well-characterized and contain a highly conserved C-terminal coiled-coil domain for plasma membrane anchoring (Perraki et al., 2012).

In plants, a spectrum of PM-bound receptor-like kinases (RLKs) are employed to coordinate signaling pathways in growth, development, and innate immunity (He et al., 2018). Several RLKs have been found to be functionally associated with remorins or flotillins (Jarsch et al., 2014). For example, the remorin protein MtSYMREM1 from the legume *Medicago truncatula*, was reported to function as a scaffolding protein mediating spatial distribution of several RLKs during symbiotic plant-microbe interactions (Lefebvre et al., 2010), including MtNFP (Arrighi et al., 2006), MtLYK3 (Smit et al., 2007), and MtDMI2 (Limpens et al., 2005). Likewise, the closest *Lotus japonicus* homolog of MtSYMREM1, LjSYMREM1 (Tóth et al., 2012), was shown to interact with the *L. japonicus* RLKs, LjNFR5 (Madsen et al., 2003), LjNFR1 (Radutoiu et al., 2003), and LjSYMRK (Stracke et al., 2002). The *Arabidopsis* flotillin protein, AtFlotillin1 (Borner et al., 2005), was shown to be critically involved in the activation of the RLK growth regulator, AtBRI1 (Russinova et al., 2004); the two proteins showed increased co-localization in response to the brassinosteroid ligand (Wang et al., 2015). More recently, Bücherl et al. (2017) observed that in *Arabidopsis*, AtBRI1 and the RLK immune receptor AtFLS2 (Gómez-Gómez and Boller, 2000) are heterogeneously but differently distributed in the membrane and that each receptor was associated with distinct remorin proteins. Despite these advances, the underlying mechanisms of compartmentalization of cell surface receptors into plasma membrane microdomains is still incompletely understood.

In this study, we set out to investigate pairwise associations between a set of representative membrane receptors, remorins and lipid-binding proteins using the BiFC assay. When RLKs such as FLS2 were ectopically co-expressed with *Solanum tuberosum* remorin StRem1.3 in *N. benthamiana* cortical cells, the BiFC fluorescent signal was heterogeneously distributed in distinct patch-like domains or nearly continuous networks across the PM. Co-localization assays suggested that these patterns may be associated with ER-PM contact sites, and thus that the BiFC complexes might unexpectedly be acting as artificial ER-PM tethering proteins. Here, using domain swap experiments involving the tether protein SYT1, we have obtained evidence that any BiFC complex that involves one integral membrane protein and one peripheral membrane protein has the potential to act as an artificial ER-PM tethering protein. This artifact has been overlooked in previous studies of membrane organization using BiFC assays.

RESULTS

Heterogeneous Patch-Like Distribution of FLS2-StRem1.3 BiFC Complexes

To provide a positive control for our studies of protein-lipid organization in the PM using BiFC, we first chose FLS2 and StRem1.3, which have been reported to co-localize with each other at the haustorial interface when FLS2 is activated by flg22 (Bozkurt et al., 2015). To do this, we fused the N-terminal fragment of Venus (VenusN) to the C terminus of FLS2, and the C-terminal fragment of Venus (VenusC) to the N terminus of StRem1.3. We also made complementary FLS2-VenusC and VenusN-StRem1.3 constructs. The pairs of BiFC constructs were ectopically co-expressed under the control the Cauliflower Mosaic Virus (CaMV) 35S promoter in *N. benthamiana* leaf cortical cells using *Agrobacterium tumefaciens*-mediated transient transformations. By confocal microscopy live-cell imaging, we observed strong BiFC fluorescence signals with both BiFC configuration pairs: FLS2-VenusN + VenusC-StRem1.3 and FLS2-VenusC + VenusN-StRem1.3 (**Figure 1**). In both configurations, the BiFC fluorescence signal was heterogeneously distributed in distinct patterns ranging from discrete patches through to continuous networks spanning the cortical surface. As a control, we co-expressed the FLS2 and StRem1.3 fusions with complementary Venus fragments that were not fused to another protein. In each case, we observed appreciable BiFC fluorescent signals (**Supplementary Figure S1**), indicating that non-specific interactions between the two fragments of Venus could occur in the absence of FLS2-StRem1.3 associations (Kodama and Hu, 2010; Gookin and Assmann, 2014). However, the BiFC fluorescence signals produced by each of these control pairs were homogenously distributed on the plasma membrane, especially in the case of FLS2. In each case, the subcellular localization closely matched that of fusions of FLS2 or StRem1.3 with full-length YFP (**Supplementary Figure S1**), indicating that the subcellular localization of each control BiFC complex was determined by the respective FLS2 or StRem1.3 component. It also indicated that the heterogeneous distribution patterns observed with the FLS2-StRem1.3 BiFC complexes were produced only when both FLS2 and StRem1.3 were present. Similar results were obtained when using YFP as the BiFC fluorophore (**Supplementary Figure S2**), or when the constructs were expressed in *Arabidopsis* mesophyll protoplasts (**Supplementary Figure S2**). When StRem1.3 was replaced by a mutant, StRem1.3* that could not bind the PM, the BiFC complexes displayed the localization expected for FLS2 alone (**Supplementary Figures S1B,C**). StRem1.3* contains mutations in the membrane-insertion loop of StRem1.3 that abolish the hydrophobicity of the loop (Perraki et al., 2012).

FLS2-StRem1.3 BiFC Complexes Appear to Localize to ER-PM Contact Sites

Since the net-like distribution of the FLS2-StRem1.3 BiFC complexes in many cells resembled the distribution of the cortical ER, we performed co-localization assays using the ER marker SP-tagRFP-HDEL (Matsushima et al., 2002). The cellular distribution of FLS2-StRem1.3 BiFC fluorescence closely

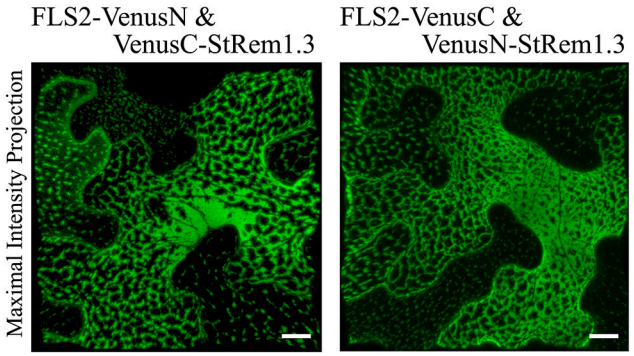

FIGURE 1 | Heterogeneous distribution of FLS2-StRem1.3 BiFC complexes in *N. benthamiana* leaf cortical cells. Examples of BiFC fluorescence signals observed after co-expression of the following pairs of constructs: FLS2-VenusN and VenusC-StRem1.3; FLS2-VenusC and VenusN-StRem1.3. Scale bars represent 10 μm.

followed the distribution patterns of SP-tagRFP-HDEL, namely net-like and sheet-like patterns of fluorescence (**Figure 2A**). We also commonly observed dynamic movements of the ER network (Stefano et al., 2014) when SP-tagRFP-HDEL was expressed alone (**Figure 2B**, **Supplementary Movie S1**). We documented the dynamic movements of the labeled organelles by using kymographs, in which the fluorescent signal along a transect is imaged over time. As shown in **Figure 2B**, the dynamic movements of the ER network labeled by SP-tagRFP-HDEL produced a chaotic kymograph. In contrast, we observed that the puncta of the FLS-StRem1.3 BiFC complexes were relatively static, producing straight lines on the kymograph (**Figure 2B**, **Supplementary Movie S2**). Moreover, in cells co-expressing both FLS2-StRem1.3 BiFC complexes and SP-tagRFP-HDEL, the puncta of the FLS2-StRem1.3 BiFC complexes co-localized with SP-tagRFP-HDEL at junctions in the ER network where the SP-tagRFP-HDEL signal showed increased stability (**Figure 2C**). However, small portions of the ER networks that were not co-localized with FLS2-StRem1.3 complexes still showed dynamic movements (**Figure 2C**). Since ER-PM contact sites are sites of reduced mobility of the ER (Henne et al., 2015), we hypothesized that the FLS2-StRem1.3 puncta may correspond to ER-PM contact sites.

To test whether the FLS2-StRem1.3 puncta may correspond to ER-PM contact sites, we co-expressed tagRFP-tagged SYT1 protein from *Arabidopsis*, which has been well-characterized as a tethering protein for ER-PM contact sites (Pérez-Sancho et al., 2015). As shown in **Figure 2D**, FLS2-StRem1.3 BiFC signals were clearly co-localized with SYT1. Moreover, a characteristic property of ER-PM junctions in mammalian cells is that they restrict the distribution of other membrane proteins in mammalian cells (Carrasco and Meyer, 2011). Though the exclusion of membrane proteins by ER-PM junctions has not been reported on plants, when we examined the distribution of membrane-associated protein AtFlotillin1 (**Supplementary Figure S3E**), reduced distribution in regions of the membrane displaying either SYT1-YFP or especially the FLS2-StRem1.3 complexes was apparent, as revealed by both maximum intensity projection and orthogonal projection (**Supplementary Figures S3B,D**) whereas general membrane labeling by FM4-64 was not restricted (**Supplementary Figures S3A,C**).

StRem1.3 and Other Peripheral Membrane Proteins Can Replace the C-Terminus of SYT1 in ER-PM Tethering

The ER-PM tethering protein SYT1 contains an N-terminal ER transmembrane domain (SYT1n) and a C-terminal peripheral PM-binding C2AC2B domain (Prinz, 2014; **Figure 3A**). As shown in **Figure 3B**, formation of a Venus BiFC complex was sufficient to reconstitute the membrane tethering function of the separated SYT1 N- and C-terminal domains. The complex showed the same distribution and stability as intact SYT1 (**Figure 3C**, **Supplementary Figure S4**). Removal of the C-terminal C2AC2B domain of SYT1 resulted in a dynamic net-like distribution, whether the SYT1 N-terminus was labeled with full length YFP (**Figure 3D**, **Supplementary Figure S4**) or a Venus BiFC complex (**Figure 3E**). This dynamic distribution co-localized with the ER marker SP-tagRFP-HDEL (**Supplementary Figure S4**). However, adding StRem1.3 to the C-terminus of SYT1n via a BiFC complex was sufficient to restore the stable ER-PM site distribution (**Figure 3F**) and could also partially stabilize the distribution of co-expressed SP-tagRFP-HDEL (**Supplementary Figure S4**). When StRem1.3 was replaced by the mutant StRem1.3*, the ability to reconstitute ER-PM tethering with SYT1n was abolished (**Figure 3G**). In addition, to reduce the possibility that tethering is an artifact of over-expression in the *N. benthamiana* transient system, we examined different times of expression. As shown in **Supplementary Figure S5**, protein fluorescence was barely visible at 18 hours post infiltration (hpi). At the earliest time point when there was sufficient expression for reliable fluorescence imaging (36 hpi), the distribution patterns were the same as at the later time point of 72 hpi, both for SYT1n-VenusN + VenusC-SYT1-C2AC2B and for SYT1n-VenusN + VenusC-StRem1.3.

To test if other peripheral membrane proteins could also participate in ER-PM tethering, we replaced the C2AC2B domain of SYT1 with the well-studied receptor-like cytoplasmic kinases (RLCKs), BIK1 (Lu et al., 2010), PBS1 (Qi et al., 2014), or CPK21 (Asai et al., 2013); these three proteins are targeted to the PM by either by N-terminal myristoylation, palmitoylation or both (**Supplementary Figure S6**). Co-expression of BIK1-VenusN + SYT1n-VenusC, PBS1-VenusN + SYT1n-VenusC, and CPK21-VenusN + SYT1n-VenusC all produced stable puncta-like distributions resembling ER-PM tethering (**Supplementary Figure S6**), which was further confirmed by co-localization analysis using SYT1 fused with tagRFP (**Supplementary Figure S6**).

Integral Membrane Proteins Can Contribute ER Anchoring to Produce ER-PM Tethering

Integral membrane proteins (IMPs) such as FLS2 are synthesized on the ER, with the N-terminal domain in the lumen of

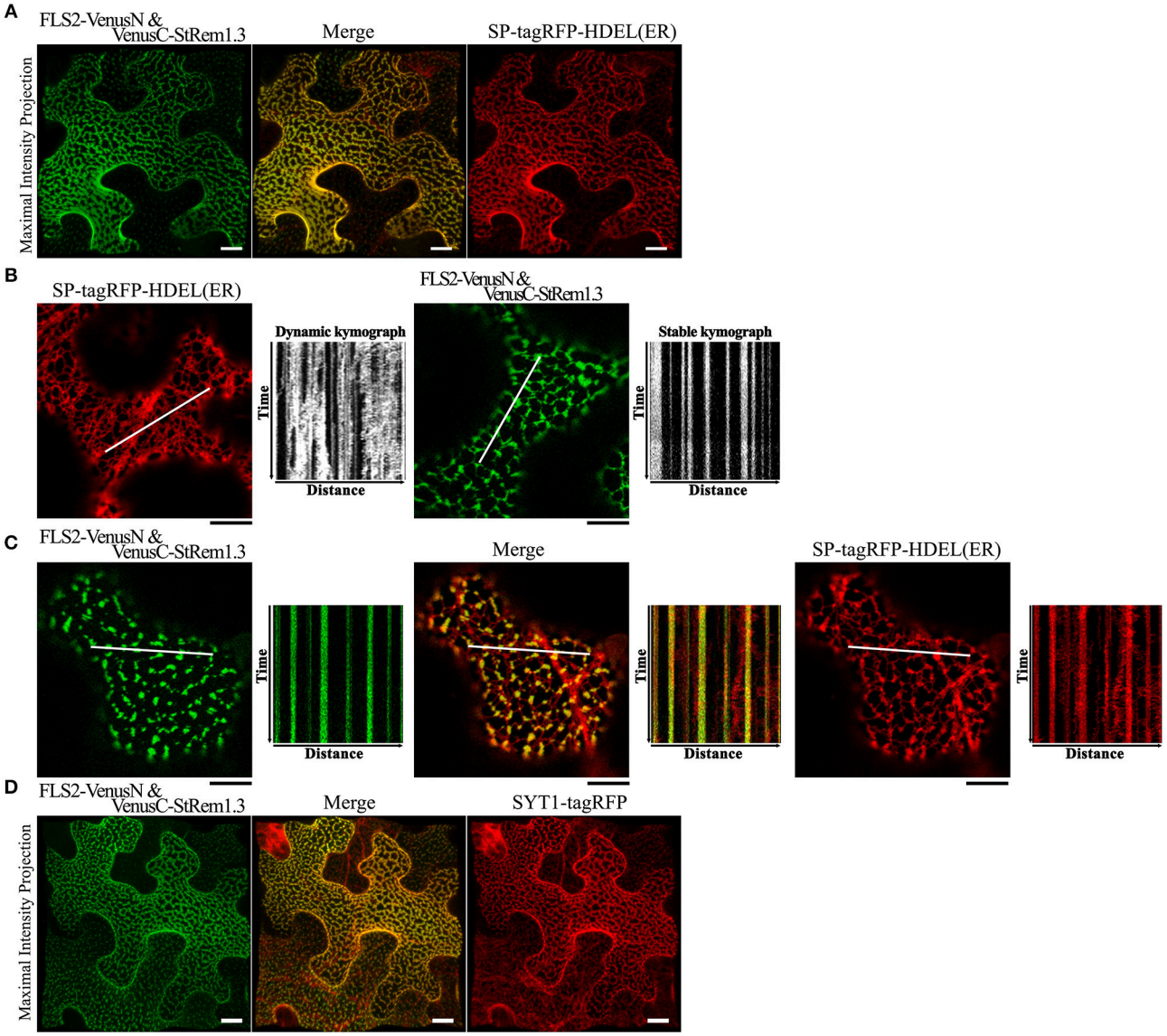

FIGURE 2 | FLS2-StRem1.3 BiFC complexes appear to associate with ER-PM contact sites in *N. benthamiana* leaf cortical cells. **(A)** FLS2-StRem1.3 BiFC complexes co-expressed with endoplasmic reticulum maker SP-tagRFP-HDEL. **(B)** Dynamic motion of the ER network labeled by ER SP-tagRFP-HDEL and stable localization of puncta of FLS2-StRem1.3 BiFC complexes revealed by kymograph analysis. **(C)** Kymograph analysis of FLS2-StRem1.3 BiFC complexes co-expressed with SP-tagRFP-HDEL. In **(B,C)**, kymographs were created from a short time-lapse series (80 s) across transect lines ~30 μm in length (shown in white). **(D)** FLS2-StRem1.3 BiFC complexes co-expressed with *Arabidopsis* ER-PM tethering protein Synaptogamin 1 (SYT1) fused to tagRFP. All scale bars (white in **A,D**; black in **B,C**) represent 10 μm.

the ER and the C-terminal domain in the cytoplasm (Walter and Johnson, 1994; Goder and Spiess, 2001). We hypothesized that the reason that FLS2 could participate in tethering-like complexes was because the formation of the FLS2-StRem1.3 complex trapped FLS2 in the ER, with its C-terminal-attached VenusN or VenusC fragment in the cytoplasm, bound to the StRem1.3 component (**Figure 4A**). As demonstrated above (**Figure 1**), StRem1.3 can contribute the PM-binding required for ER-PM tethering, while the StREM1.3* mutant that lacks PM-binding cannot (**Supplementary Figure S1B**). Thus we inferred that binding of the StRem1.3 component to the PM could trap the FLS component in the ER.

To address whether other IMPs could also form this ER-PM tethering structure with StRem1.3 through BiFC self-assembly, we selected several well-studied plasma membrane RLKs which share similar structural characteristics with FLS2 and also have similar localization patterns (**Supplementary Figure S7**). RLKs are integrated into the ER through the co-translational translocation machinery. We selected EF-Tu receptor (EFR) (Zipfel et al., 2006), brassinosteroid-associated kinase (BAK1)

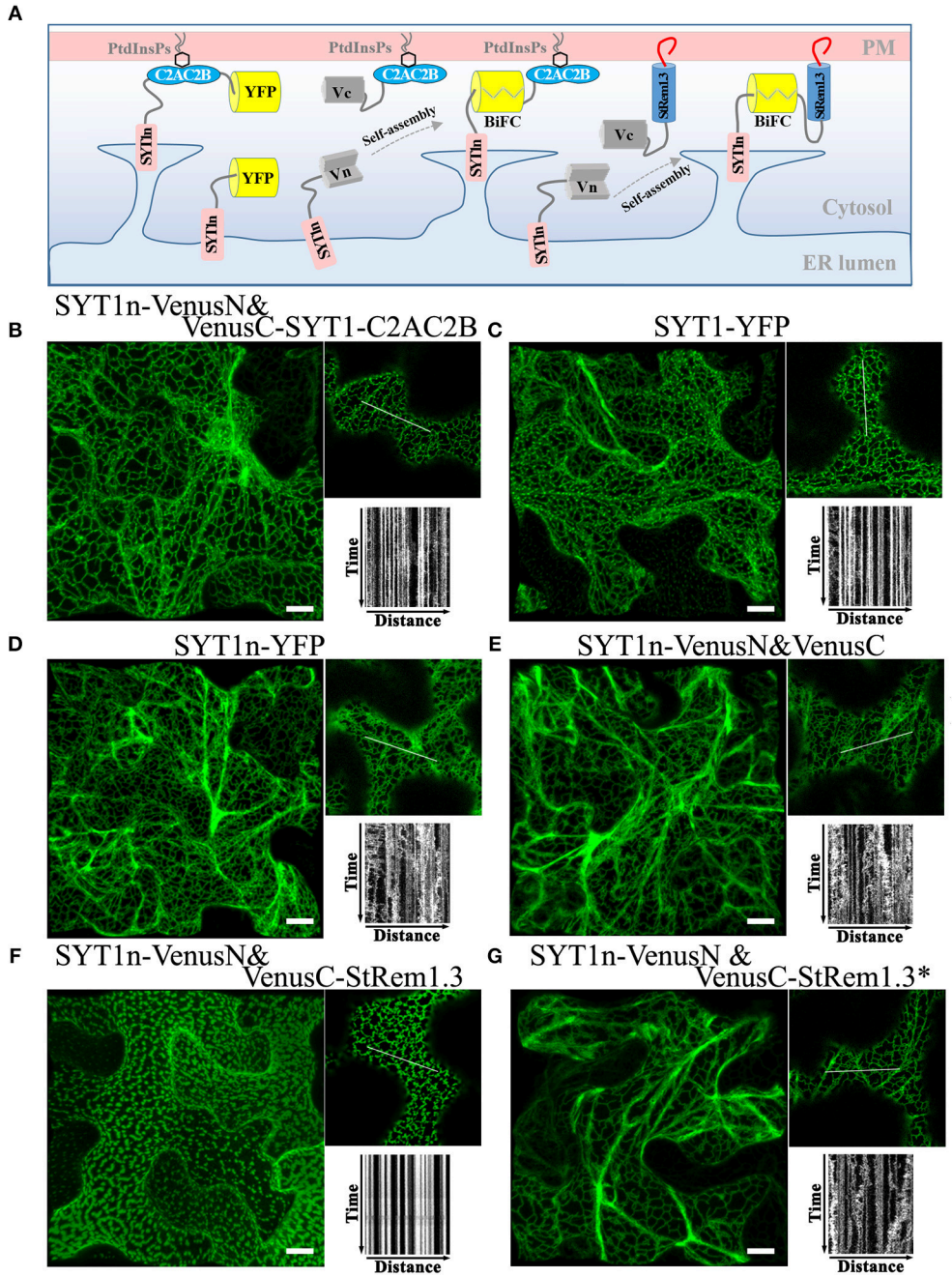

FIGURE 3 | A C-terminal peripheral PM-binding domain is required for ER-PM tethering by *Arabidopsis* SYT1 in *N. benthamiana* leaf cortical cells. **(A)** Explanatory schematic of reconstitution of SYT1 ER-PM tethering using BiFC complexes. **(B,C)** Distribution and kymograph analysis of full length SYT1 or SYT1 reconstituted using Venus BiFC complexes. **(D,E)** Distribution and kymograph analysis of SYT1 lacking the C-terminal peripheral PM-binding domain C2AC2B labeled by either full-length YFP or a free Venus BiFC complex. **(F,G)** Distribution and kymograph analysis of SYT1n fused to WT-type StRem1.3 or PM-non-binding mutant StRem1.3* via Venus BiFC complexes. All kymographs were created as described in **Figure 2**. All scale bars represent 10 μm.

(Heese et al., 2007), BRI1 (Russinova et al., 2004), and ERECTA receptor (ERec) (Bemis et al., 2013). When co-expressed with StRem1.3 in BiFC complexes, all these RLKs produced stable distribution patterns consistent with ER-PM tethering (**Figure 4B**).

Next we tested IMPs that insert into the ER membrane post-translationally. For this purpose we selected tail-anchored (TA) proteins. These proteins lack an N-terminal signal peptide but contain a single transmembrane domain (TMD) which resides so close to the C terminus that it cannot

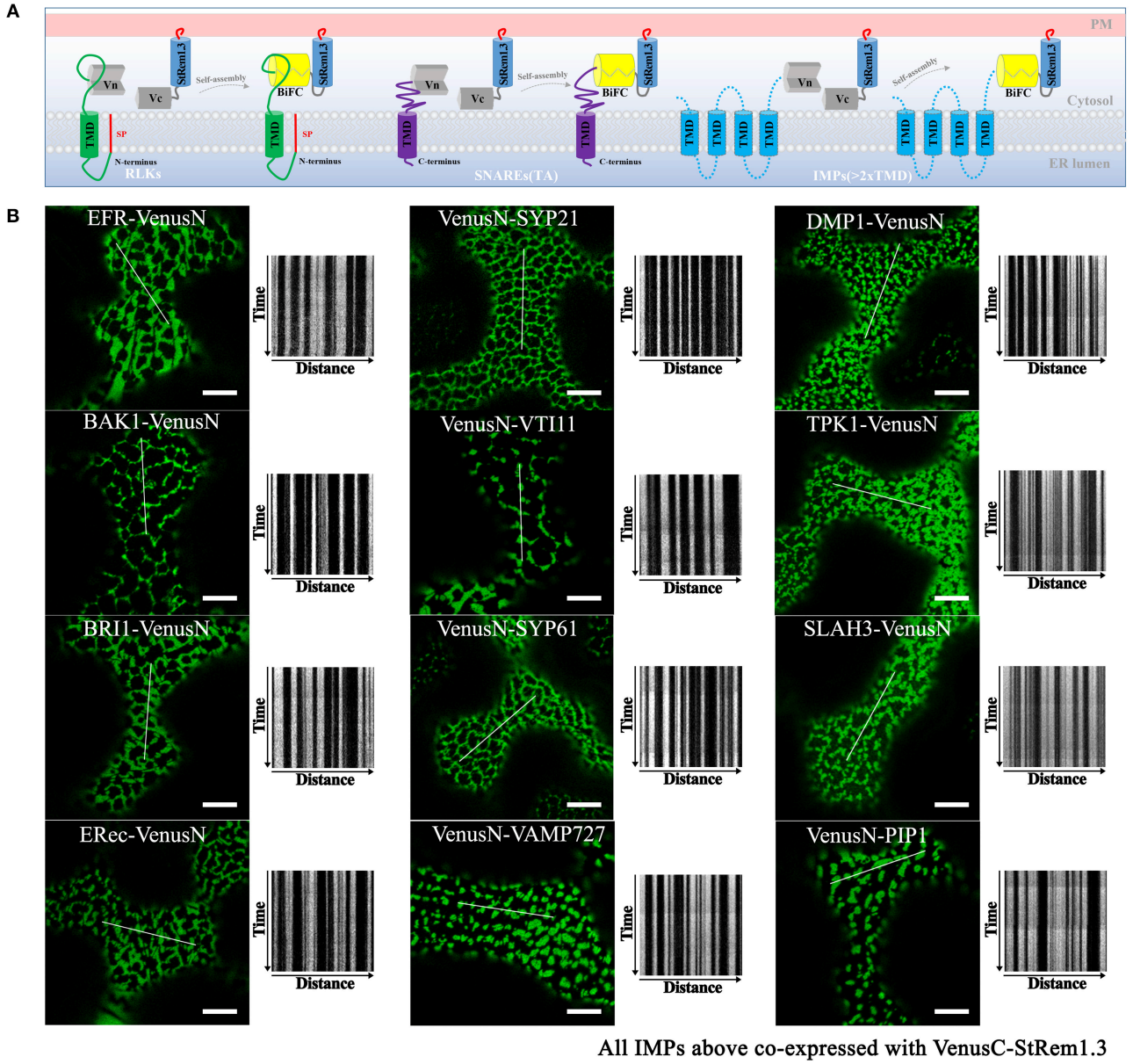

FIGURE 4 | Integral membrane proteins co-expressed with StRem1.3 in Venus BiFC complexes produce EM-PM tethering in *N. benthamiana* leaf cortical cells. **(A)** Explanatory schematic of representative classes of IMPs tested: IMPs with a cleavable N-terminal signal peptide and single-pass TMD; C-terminally anchored IMPs with single-pass TMD (tail-anchored SNARE proteins); IMPs with multi-pass TMDs. **(B)** Localization and kymograph analysis of Venus BiFC complexes formed with each IMP and StRem1.3. All kymographs were created as described in **Figure 2**. All scale bars represent 10 μm.

be recognized by the signal recognition particle (SRP) (Rapoport, 2007; Hegde and Keenan, 2011). We selected a set of *Arabidopsis* TA SNARE proteins, namely SYP21 (Qa-SNARE) (Foresti et al., 2006), VTI11 (Qb-SNARE) (Sanmartín et al., 2007), SYP61 (Qc-SNARE) (Hachez et al., 2014), and VAMP727 (R-SNARE) (Ebine et al., 2008). In these proteins, the C-terminal TMD determines their localization in vesicles of the secretory and endocytic pathways (**Supplementary Figure S7**). In each case, co-expression of these TA SNARE proteins with StRem1.3 in BiFC complexes resulted in a stable distribution consistent with ER-PM tethering (**Figure 4B**).

We also tested several IMPs which span the membrane bilayer more than once, that reside on the PM, endosomal membranes, and vacuolar membrane (**Supplementary Figure S7**). We tested *Arabidopsis* DUF679 membrane protein (AtDMP1) (Kasaras et al., 2012), tonoplast potassium channel protein AtTPK1 (Maîtrejean et al., 2011), slow anion channel 1 (SLAC) homolog SLAH3 (Demir et al., 2013), and intracellular aquaporin PIP1 (Wudick et al., 2009). As shown in **Figure 4B**, a pattern consistent

with ER-PM tethering was observed when each of the multi-pass IMPs was co-expressed with StRem1.3 in BiFC complexes. Together, the above results suggest that patterns consistent with ER-PM tethering were produced with multiple types of IMPs.

Additionally, observations of FLS2, SYP21, or AtDMP1 BiFC complexes formed with StRem1.3 after different times of expression or in cells with different expression levels suggested that the formation of tethering complexes was not an artifact of over-expression (**Supplementary Figure S8**). While the complexes were barely visible at 18 hpi, the patterns at 36 hpi (the earliest time when visualization was reliable) were almost identical as at 72 hpi. Cells with low levels of BiFC complex formation generally exhibited discrete punctae resembling EPCSs, while in cells with higher levels, the punctae were larger and in some cases merged to form network patterns (**Supplementary Figure S8**).

In contrast to the IMPs, we did not observe distributions consistent with ER-PM tethering when peripheral membrane proteins were paired with StRem1.3 in BIFC complexes. BIK1-VenusN, PBS1-VenusN, and CPK21-VenusN co-expressed with VenusC-StRem1.3, produced only homogeneously distributed BiFC signals on the PM (**Supplementary Figure S9**). Similar results were also obtained with *Arabidopsis* SNAP33 (Kargul et al., 2001; Jahn and Scheller, 2006) which has been recognized as a membrane targeted Qbc-SNARE protein lacking a TMD (**Supplementary Figure S9**). Collectively, these results imply at least one IMP is required in the BiFC complex to produce ER-PM tethering.

PtdIns(4)P- and PtdIns(4,5)P_2-Binding Proteins Could Replace Peripheral Membrane-Binding Proteins in BiFC Complexes to Produce ER-PM Tethering

SYT1 normally binds acidic phospholipids in the PM via a C2 domain (Pérez-Sancho et al., 2015; **Figure 3**). Pleckstrin homology (PH) domains are a large family of phosphoinositide-binding proteins with a broad range of specificities (Lemmon, 2008). Fluorescent protein-tagged PH domain proteins have been used in plants and other organisms to detect PtdIns(4)P and PtdIns(4,5)P_2 In plants, the PM has been identified as a pool for both PtdIns(4)P and PtdIns(4,5)P_2 (Van Leeuwen et al., 2007; Vermeer et al., 2009). We therefore tested whether PtdIns(4)P and PtdIns(4,5)P_2 binding PH domain proteins could replace the C2 domains of SYT1 for ER-PM tethering. We used the PH domains of the PtdIns(4)P-binding protein FAPP1 (Dowler et al., 2000), and of the PtdIns(4,5)P_2 binding protein PLC-delta 1 (Yagisawa et al., 1998); both have been well-characterized in animal cell systems and have been used in plants previously (Van Leeuwen et al., 2007; Vermeer et al., 2009; Simon et al., 2016). In the case of FAPP1, we used a mutant of FAPP1 (E50A, H54A; hereafter named FAPP1a) that no longer binds the golgi protein ARF1 (Simon et al., 2016). As a negative binding control, we designed site-directed mutants of each biosensor lacking lipid binding based on previous reports (Yagisawa et al., 1998; He et al., 2011). To begin with, we performed subcellular localization assays on YFP-tagged SYT1-C2AC2B, FAPP1a-PH, FAPP1a-PH*, PLCδ1-PH, and PLCδ1-PH* (*indicates the mutants). Similar to the results previously observed for C2AC2B-GFP (Pérez-Sancho et al., 2015), YFP-$PH^{FAPP1-E50A-H54A}$ (Simon et al., 2016), and YFP-$PH_{PLC\delta1}$ (Van Leeuwen et al., 2007), we observed that FAPP1a-PH-YFP was more strictly localized at the PM than YFP-SYT1-C2AC2B and PLCδ1-PH-YFP, which additionally displayed cytosolic and nuclear localizations (**Figure 5A**). In contrast, both the FAPP1a-PH* and PLCδ1-PH* mutants showed diffuse patterns of cytosolic localization (**Figure 5A**). When co-expressed with SYT1n-VenusN, all three of VenusC-SYT1-C2AC2B, VenusC-FAPP1a-PH, and PLCδ1-PH-VenusC showed patterns consistent with ER-PM tethering (**Figure 5B**), while the mutant PH domains produced only dynamic patterns associated with ER localization (**Figure 5B**). In contrast, when the PtdIns(3)P-binding protein domains, VAM7-PX (Cheever et al., 2001) or Hrs-2xFYVE (Vermeer et al., 2006), were provided as potential PM-binding proteins, only dynamic ER localization patterns were observed (**Supplementary Figure S10**), comparable to the FAPP1a-PH* and PLCδ1-PH* mutants. Furthermore, PtdIns(3)P-non-binding mutants of VAM7-PX and Hrs-2xFYVE, which were designed according to previously identified binding sites (Kutateladze and Overduin, 2001; Lee et al., 2006; Pankiv et al., 2010), produced distribution patterns (**Supplementary Figure S10**) comparable to their wild type counterparts. Interestingly, the SYTn-PLCδ1-PH BiFC complexes produced a very fine network distribution, with well-defined puncta, that was closely similar to the pattern produced by SYTn-SYT1-C2AC2B BiFC complexes. In contrast, the SYTn-FAPP1a-PH BiFC complexes exhibited a thicker network with very abundant puncta, comparable to the patterns exhibited SYT1n-StRem1.3 BiFC complexes. We speculate that this difference may be associated with the stronger PM localization exhibited by FAPP1a-PH and StRem1.3 (**Figure 5A**, **Supplementary Figure S1**). In conclusion, our data suggest that PtdIns(4)P- and PtdIns(4,5)P_2-binding proteins, but not PtdIns(3)P-binding proteins, could contribute the PM-targeting needed for ER-PM tethering.

DISCUSSION

In this study, we observed that BiFC complexes containing both the RLK, FLS2, and the membrane-associated remorin protein, StRem1.3, exhibited a range of heterogeneous distribution patterns closely resembling those produced by over-expression of the *Arabidopsis* ER-PM tether protein, SYT1 (**Figures 1**, **2**). Indeed, co-expression of the FLS2-StRem1.3 BiFC complexes with SYT1 produced fully overlapping distributions (**Figure 2**), suggesting that the FLS2-StRem1.3 BiFC complexes might act as artificial ER-PM tethering proteins (**Figure 6**). Since the gap between the ER and the PM is in the 15–20 nm range (McFarlane et al., 2017) and therefore is too small to be resolved by light microscopy (diffraction limit), we used the stability of tethering sites to distinguish them from the more dynamic free ER networks, using kymographs. We note also that since we did not use electron microscopic observations, we cannot rule out that the stable puncta labeled by SYT1-FP are not true contact sites. The co-location of SYT1 with the artificial tethering sites suggests

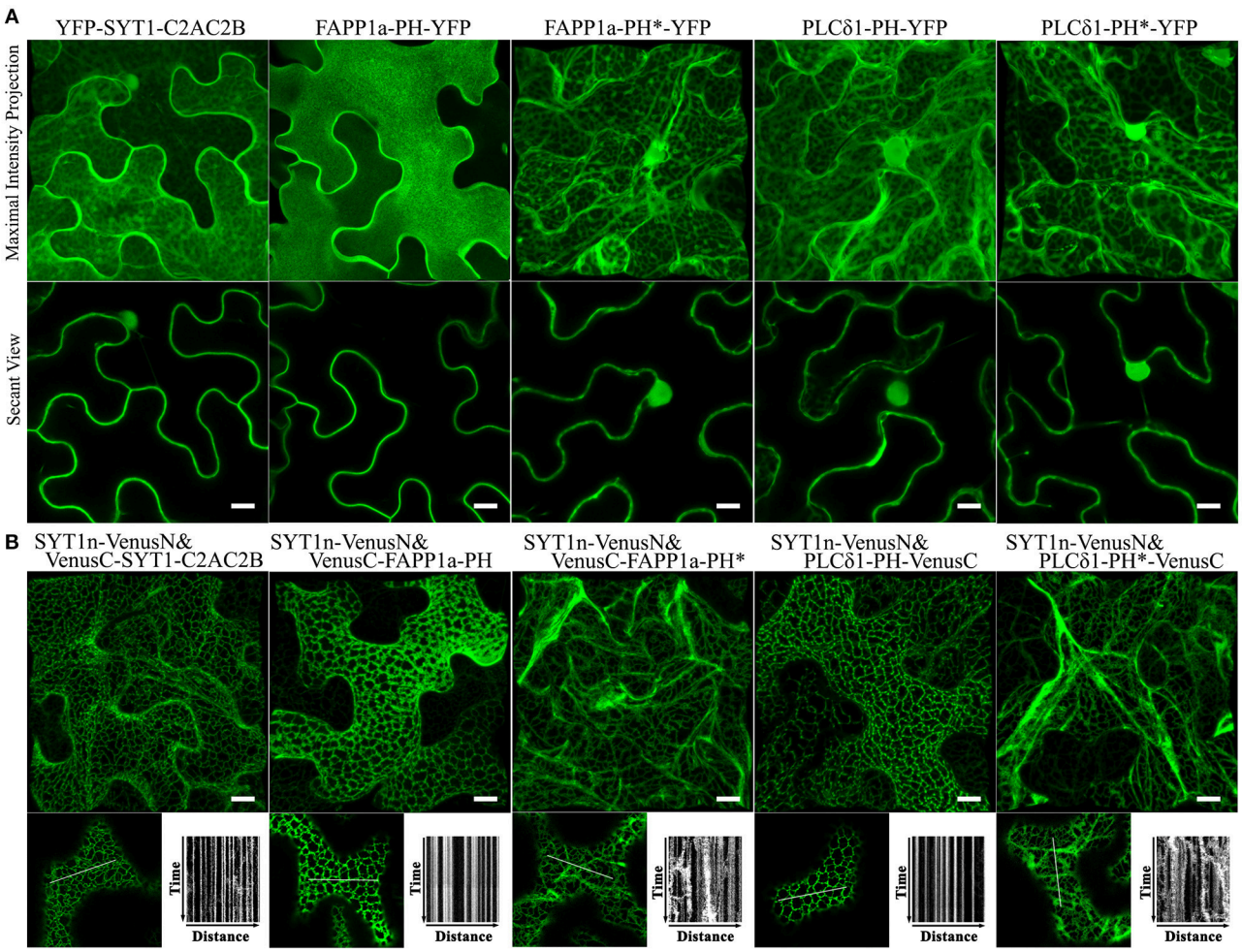

FIGURE 5 | Lipid binding proteins co-expressed with the SYT1 N-terminal domain in BiFC complexes produce EM-PM tethering in *N. benthamiana* leaf cortical cells. **(A)** Subcellular localization of YFP-fused lipid-binding domains SYT1-C2AC2B, FAPP1a-PH, and PLCδ1-PH, together with lipid-non-binding mutants FAPP1a-PH* and PLCδ1-PH*. **(B)** Localization and kymograph analysis of BiFC complexes formed from lipid binding domains and mutants fused with VenusC and co-expressed with SYT1n-VenusN. All kymographs were created as described in **Figure 2**. All scale bars represent 10 μm.

that the artificial sites might develop into true contact sites. In future, co-expressing the tethering constructs with NET3C might provide additional information about the relationship of the tethering sites we observe with bona fide contact sites (Wang et al., 2014).

We showed that StRem1.3 and also the lipid-conjugated peripheral membrane proteins BIK1, PBS1, and CPK21, could replace the PM-binding C2 domain of SYT1 (**Figure 3**, **Supplementary Figure S6**) to produce ER-PM tethering. We showed that the phosphoinositide-binding PH domains from FAPP1 and PLCδ1 could also functionally replace the C2 domain of SYT1 (**Figure 5**). Finally, we showed that a wide variety of IMPs that transit the ER, including 5 RLKs, 4 tail-anchored proteins, and 4 multi-transmembrane domain proteins, could provide the EM-anchoring function when paired with StRem1.3 as the PM-anchoring protein (**Figure 4**). In contrast, peripheral membrane proteins that do not transit the ER could not provide the ER-anchoring function (**Supplementary Figure S9**). On the basis of these observations, we have concluded that FLS2-StRem1.3 BiFC complexes may in fact act as artificial ER-PM tethering proteins. More generally, our model is that any ER-transiting IMP paired with a peripheral membrane protein, either in a BiFC complex or through a direct linkage, may act as an artificial ER-PM tethering protein (**Figure 6**). In this model, the IMP must transit through the ER, either co-translationally or post-translationally (Walter and Johnson, 1994; Goder and Spiess, 2001). Furthermore, the binding of the peripheral membrane protein to the PM should be sufficiently strong to trap the IMP in the ER, and prevent the completion of the IMP's transit to its final membrane destination. Conversely, the peripheral membrane protein should be synthesized in the cytoplasm and then be targeted to the PM post-translationally, without entering the ER, either via conjugation to a lipid, binding to a PM lipid, or via insertion of a hydrophobic

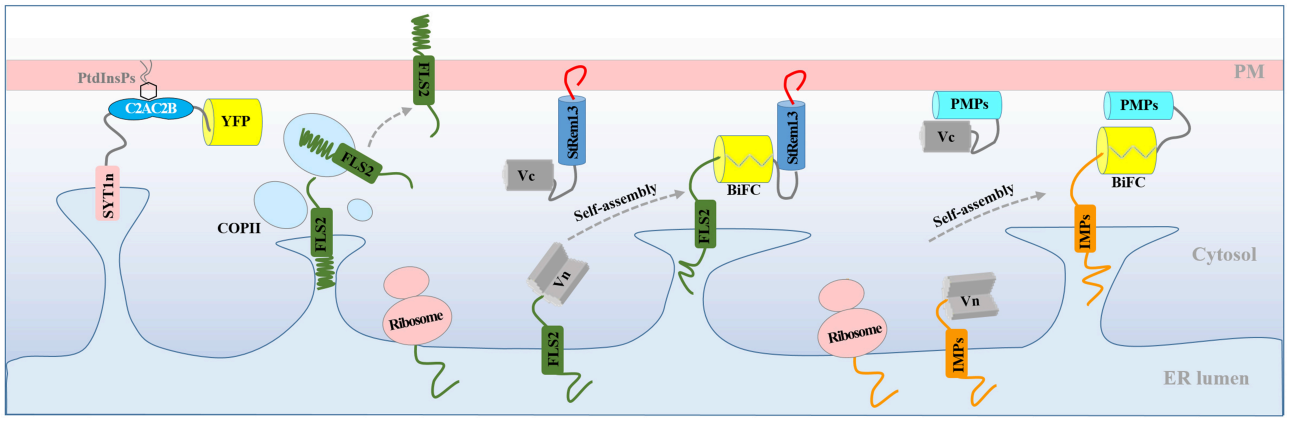

FIGURE 6 | Model for the production of ER-PM tethering complexes via BiFC. Normally, newly synthesized RLK protein FLS2 is targeted to the PM through the ER and transported to the PM via the coat protein complex II (COPII) system. Co-expression of FLS2 and StRem1.3 in BiFC constructs results in rapid spontaneous formation of Venus BiFC complexes tethered to the PM. PM tethering blocks ER-anchored FLS2 from delivery to the PM, resulting in artificial PM-ER complexes. Artificial ER-PM tethering could be created by pairing any ER-transiting integral membrane protein (IMP) with any peripheral membrane protein (PMP) in a BiFC complex.

loop or helix (Vögler et al., 2008; Pu et al., 2010; Resh, 2013; Stillwell, 2016).

In plants, several studies have reported observing heterogeneous distributions of BiFC complexes that combine IMPs with peripheral membrane proteins. However, none of these studies have considered the possibility that the distribution patterns observed may have arisen as a result of the formation of artificial ER-PM tethering proteins. For example, Jarsch et al. (2014) showed that whereas the FP-tagged RLK MtNFR1 and remorin MtSYMREM1 were uniformly distributed across the PM when individually expressed in *N. benthamiana* leaf epidermal cells, when the two were co-expressed in a BiFC complex, the fluorescent signal was exclusively observed in distinct, immobile puncta. Similarly, Demir et al. (2013) observed that BiFC complexes comprised of *Arabidopsis* SLAH3 (an IMP) and CPK21 (a PMP) localized to distinct PM puncta. Likewise, Bücherl et al. (2017) expressed the following RLK-PMP proteins pairs in BiFC complexes and observed the formation of distinct puncta on the PM: FLS2-BSK1, BRI1-BSK1, FLS2-BIK1, and BRI1-BIK1. Our data suggest that it is necessary to re-evaluate the applicability of BiFC assays for plant membrane studies, and the validity of published studies that used this approach (e.g., Demir et al., 2013; Jarsch et al., 2014; Bücherl et al., 2017) should be re-visited.

Unambiguously determining PM localization in plant cells is challenging. In comparison to mammalian cells, many plant cells contain a large central vacuole that takes up most of the cell volume, resulting in the cytoplasm and organelles being constrained into the periphery of the cell and appressed to the PM. Several methods have been commonly used to distinguish the PM from the vacuolar membrane (tonoplast), including plasmolysis (Speth et al., 2009) and osmolysis (Serna, 2005). However, these methods may be confounded by the presence of the tonoplast or of overexpression artifacts. For example, we observed that some weakly binding PMPs, e.g., SNAP33 (**Supplementary Figure S9**), SYT1-C2AC2B (**Figure 5**), and PLCδ1-PH (**Figure 5**), show substantial cytoplasmic localization when they are over-expressed as FP fusions. The ability of PMPs to form ER-PM tethering complexes may in some circumstances aid in distinguishing between cytosolic and membrane proteins. For example, there is currently not a strong consensus as to the localization of PtdIns(4,5)P_2 in plant cells (Delage et al., 2012). Although PtdIns(4,5)P_2 has been well established as a PM lipid in animal cells (Hammond et al., 2012), evidence for the same localization in plant cells has been ambiguous (Van Leeuwen et al., 2007). Our observations that PLCδ1-PH is effective in forming ER-PM tethering complexes with SYT1n suggests that PtdIns(4,5)P2 is indeed located in the plant PM (but does not rule out other locations as well). In contrast, our negative tethering results with PtdIns(3)P-binding proteins suggest that this lipid does not reside on the cytoplasmic face of the PM.

Given the ability of IMPs to act as the ER-anchor in artificial ER-PM tethering complexes, such complexes could possibly be used to investigate whether a protein may be an IMP or not, as suggested previously by Zamyatnin et al. (2006). Bioinformatic analysis has been increasingly used to predict the identity and topology of IMPs. However, these algorithms are not fully accurate. For example, two commonly used programs TMHMM (Krogh et al., 2001) and Protter (Omasits et al., 2014) can differ in their predictions. Artificial ER-PM tethering complexes could be used to test such predictions. As one example from this work, Protter and TMHMM both predicted a weak TMD in CPK21 whereas all other members of the CDPK family are targeted to the PM by myristoylation and palmitoylation (Speth et al., 2009; Asai et al., 2013; Schulz et al., 2013), suggesting that the bioinformatic prediction may be incorrect. In fact, we observed that CPK21-SYT1n BiFC complexes exhibited tethering (**Supplementary Figure S6**) but CPK21-StRem1.3 BiFC complexes did not (**Supplementary Figure S9**), confirming CPK21 as a PMP, not an IMP. Further examples will be needed to determine if this approach is generally useful.

Genetically designed chimeric proteins have been successfully developed to manipulate tethering of the ER to the PM or to other organelles, and to study cellular processes involving tethering proteins (Kornmann et al., 2009; Chang et al., 2013; Bockler and Westermann, 2014; Poteser et al., 2016; Lee et al., 2019). For example, a chimeric protein named MAPPER was used as a constitutive ER-PM tethering marker to investigate the molecular mechanism for dynamic regulation of ER-PM tethering during Ca^{2+} signaling in live mammalian cells; MAPPER is derived from the human ER-PM tether STIM1 and contains minimal ER and PM-targeting motifs, linked by a fluorescent protein (Chang et al., 2013; Poteser et al., 2016). More recently, MAPPER has also been used as a non-regulated ER-PM tethering marker to study the response of *Arabidopsis* SYT1 on the regulation of ER-PM connectivity under ionic stress (Lee et al., 2019). Additionally, ChiMERA, a synthetic ER-Mitochondria tether consisting of GFP fused to the mitochondrial membrane anchored TMD motif of Tom70 and an ER tail-anchor motif from Ubc6, was used to restore mitochondria-ER contacts in yeast mutants (Kornmann et al., 2009; Bockler and Westermann, 2014). Therefore, our work here not only suggests a potential way to develop fluorescent molecular markers for EPCSs, but also suggests a molecular tool to manipulate tethering of the ER to the PM, or even to other membrane organelles in plants. One can imagine, for example, tethering complexes in which dimerization of the two components is regulated by small molecules and/or light as reported previously (Karginov et al., 2011; Guntas et al., 2015).

In summary, we have deployed an extensive toolset of plant membrane marker proteins and mutant controls (summary in **Table 1**, **Supplementary Table S1**) to characterize the artificial ER-PM tethering that may result from spontaneous reassembly of fragmented fluorescent proteins during co-localization studies. These results complement our findings that a similar phenomenon can produce tethering of multi-vesicular bodies and the tonoplast to the PM (Tao et al., 2019). Our results indicate the possibility of new tools for deliberately manipulating ER-PM tethering, while at the same time highlighting a previously unrecognized artifact that may have confounded several published studies.

EXPERIMENTAL PROCEDURES

Plant Materials

Nicotiana benthamiana and *A. thaliana* plants were grown in soil (Fafard® 4M Mix). *N. benthamiana* plants were grown in a growth chamber with a 14 h photoperiod at 25°C for 5 weeks before *A. tumefaciens* infiltration assays. *A. thaliana* seeds were sown in soil and left at 4°C for 3 day of cold stratification. Then the seedlings were grown in a growth chamber with a 12 h photoperiod at 20°C for 4 weeks before protoplast isolation.

Cloning and Construction

FLS2, BAK1, BRI1, ER, BIK1, PBS1, FAPP1-PH, Hrs-2xFYVE, VAM7-PX were sub-cloned from constructs described previously (Kale et al., 2010; Lu et al., 2010; Meng et al., 2015). The SYT1 (AT2G20990.1), AtDMP1 (AT3G21520.1), AtTPK1 (AT5G55630.1), AtPIP1 (AT3G61430.1), SLAH3 (AT5G24030.1), CPK21 (AT4G04720.1), SNAP33 (AT5G61210.1), AtSYP21 (AT5G16830.1), AtVTI11 (AT5G39510.1), AtVAMP727 (AT3G54300.1), AtSYP61 (AT1G28490.1), AtFlotillin1 (AT5G25250) coding regions were amplified from *Arabidopsis* Col-0 cDNA. StRem1.3 (U72489.1), and PLCδ1-PH (BC050382.1) were synthesized by GenScript Corporation. All PCR amplifications were performed by High-Fidelity DNA polymerase (CloneAmpTM HiFi PCR Premix, TaKaRa Bio). All PCR products were individually recombined by In-Fusion® HD Cloning (TaKaRa Bio) into the Gateway vector pDONR207 into which VenusN, YFPn, VenusC, YFPc, or full-length FPs had previously been inserted. The ER marker was generated by using PCR mutagenesis to add a carboxyl-terminal HDEL peptide to tagRFP, then cloning tagRFP-HDEL into a vector (psAEV) that provided a signal peptide. The site-specific mutations of PLCδ1-PH*, StRem1.3*, FAPP1a-PH*, VAM7-PX*, and Hrs-2xFYVE* were introduced into their respective pDONR207 constructs using appropriate oligonucleotides in a PCR reaction that amplified the entire vector. A list of primers designed and used are in **Supplementary Table S2**. By using the Gateway® LR reaction (Thermo Fisher scientific Inc.), all constructs were transferred from their pDONR207 vectors into the destination expression vectors namely pmAEV, which is derived from binary vectors pCAMBIA (Dou et al., 2008) and driven by the Cauliflower Mosaic Virus (CaMV) 35S promoter conferring constitutive high level expression in plant cells. All these plasmid constructs were confirmed by DNA sequencing at the Center for Genome Research and Biocomputing (Oregon State University).

Transient Expression in *N. benthamiana* Leaves and *A. thaliana* Protoplasts

The procedures to introduce expression vectors into *A. tumefaciens* strain GV3101, and to infiltrate transformed *A. tumefaciens* cells into 5-week-old *N. benthamiana* leaves were carried out as described previously (Lu et al., 2013). *A. tumefaciens* cells were infiltrated at OD_{600} of 0.1 for the expression of the full-length fluorescent protein tagged proteins; for co-expression of BiFC constructs, two *A. tumefaciens* cultures with OD_{600} of 0.2, respectively, were equally mixed together to reach the final OD_{600} at 0.1. All infiltrated *A. tumefaciens* cells were suspended in MES buffer (10 mM $MgCl_2$, 10 mM MES pH 5.7, and 100 μM acetosyringone). *N. benthamiana* leaves were imaged at 3 days post infiltration. *A. thaliana* mesophyll protoplasts were prepared from leaves of 4-week-old seedlings, and 10 μg of plasmid DNA were used for each transformation as described (Yoo et al., 2007). Following transformation, protoplasts were suspended overnight in W5 buffer (154 mM NaCl, 125 mM $CaCl_2$, 5 mM KCl, 2 mM MES pH 5.7) at 25°C before observation.

Live-Cell Imaging by Confocal Microscopy and Image Analysis

FM 4-64 (ThermoScientificBio) staining employed a concentration of 10 μM, and was performed as previously

TABLE 1 | Fluorescent marker proteins and mutants used in this study.

Protein	Accession/Tair	Region	Localization in *N. benthamiana* leaf cortical cells	Features	References
SUBCELLULAR MARKERS					
FLS2	AT5G46330.1	FL	PM	IMP	Gómez-Gómez and Boller, 2000
StRem1.3	NP_001274989	FL	PM	PMP	Perraki et al., 2012
StRem1.3*		FL	Cytoplasm, nuclear	C terminal mutations eliminating PM-binding L179H, A180H, A181H, Y184S, A185S, G187V, A189A, L194S, G195Q, I196Q, F197Q	Perraki et al., 2012
SYT1	AT2G20990	FL	ER-PM tether	IMP	Pérez-Sancho et al., 2015
SYT1n	AT2G20990	1–243	ER membrane	N-terminal domain of SYT1	Pérez-Sancho et al., 2015
SYT1-C2AC2B	AT2G20990	244–541	PM (mainly), cytoplasm, nuclear	C-terminal domain of SYT1 binding to a variety of negatively charged phospholipids	Pérez-Sancho et al., 2015
AtFlotillin1	AT5G25250	FL	PM	PMP	Jarsch et al., 2014
BIK1	At2g39660	FL	PM	PMP	Lu et al., 2010
PBS1	AT5G13160	FL	PM	PMP	Qi et al., 2014
CPK21	AT4G04720	FL	PM	PMP	Asai et al., 2013
EFR	AT5G20480	FL	PM	IMP	Zipfel et al., 2006
BAK1	AT4G33430.1	FL	PM, though slight cell death observed	IMP	Heese et al., 2007
BRI1	AT4G39400.1	FL	PM	IMP	Russinova et al., 2004
ERec	AT2G26330.1	FL	PM	IMP	Bemis et al., 2013
SYP21	AT5G16830	FL	MVB, tonoplast	IMP	Foresti et al., 2006
VTI11	AT5G39510	FL	Golgi, MVB, tonoplast	IMP	Sanmartín et al., 2007
SYP61	AT1G28490	FL	TGN/EE	IMP	Hachez et al., 2014
VAMP727	AT3G54300	FL	Endosomal organelles (partially MVBs), tonoplast	IMP	Ebine et al., 2008
SNAP33	AT5G61210	FL	PM (not visible by regular FP-tagged localization analysis), cytoplasm (mainly), nuclear	PMP	Kargul et al., 2001
AtDMP1	AT3G21520.1	FL	MVBs, tonoplast (mainly)	IMP (GFP inserted between 108E and 109P)	Kasaras and Kunze, 2017
AtTPK1	AT5G55630	FL	MVBs, tonoplast (mainly)	IMP	Maîtrejean et al., 2011
PIP1	AT2G36830	FL	Endosomal organelle	IMP	Wudick et al., 2009
FAPP1a-PH	AAG15199	1–99	PM	FAPP1-PH protein containing mutations of the ARF1 binding site: E50A, H54	He et al., 2011
FAPP1a-PH*		1–99	Cytoplasm, nuclear	Mutations of PtdIns(4)P binding site K7E, R18A	He et al., 2011
PLCδ1-PH	AAH50382	1–174	PM (not visible by regular FPs-tagged localization analysis), cytoplasm (mainly), nuclear	PtdIns(4, 5)P binding	Yagisawa et al., 1998
PLCδ1-PH*		1–174	Cytoplasm, nuclear	Mutations of PtdIns(4,5)P binding site K30A, K32E, R40A	Yagisawa et al., 1998
tagRFP-HDEL			The lumen of endoplasmic reticulum	Includes Ssignal peptide (MGYMCIKISFCVMCVLGLVIVGDVAYA) cloned from soybean (Glycine max) secreted protein PR1a precursor (Accession: NP_001238168)	Matsushima et al., 2002
SLAH3	AT5G24030	FL	PM	IMP	Demir et al., 2013
VAM7-PX	NP_011303	1–134	MVBs, tonoplast	PtdIns(3)P binding	Kale et al., 2010
VAM7-PX*		1–134	Cytoplasm, nuclear	Mutations of PtdIns(3)P binding site R40E, S42A	Lee et al., 2006
Hrs-2xFYVE	NP_032270	147–223	MVBs, tonoplast	Tandem repeat of PtdIns(3)P binding domain, linked by QGQGS	Vermeer et al., 2006
Hrs-2xFYVE*		147–223	Cytoplasm, nuclear	Mutations of both PtdIns(3)P binding sites R34S, K35S, H36S, H37S, R39S	Kutateladze and Overduin, 2001; Pankiv et al., 2010

**mutant; ER, endoplasmic reticulum; FL, full length; IMP, integral membrane protein; MVB, multivesicular bodies; PM, plasma membrane; PM-MVB/TP, plasma membrane-multivesicular body/tonoplast tethering sites; PMP, peripheral membrane protein; SP, signal peptide; tagRFP, tag red fluorescent protein; TP, tonoplast; YFP, yellow fluorescent protein.*

described (Günl et al., 2011). All microscopy images were obtained using a ZEISS LSM 780 NLO confocal microscope system equipped with a 458-nm argon laser for CFP (emission wavelength 560–509 nm), a 514-nm argon laser for YFP/Venus (emission wavelength 518–553 nm), and a 561-nm Diode Pumped Solid State (DPSS) laser for tagRFP and FM4-64 (emission wavelength 562–640 nm). For time-lapse imaging, 100 consecutive frames without time intervals (combined speed of about 0.78 fps) were acquired sequentially. The kymograph plots were generated using ImageJ (Version 1.51n, NIH) and the plug-in "KymographBuilder" with a 30 μm segmented line for this measurement. When interpreting the kymographs, close attention was paid to distinguishing the cortical ER from transvacuolar strands, which are also dynamic. All microscopy images were processed using the Zeiss ZEN2 (Blue edition) program.

AUTHOR CONTRIBUTIONS

KT and BT conceived and planned the experiments and wrote the manuscript. KT performed experiments and analyzed the data. JW and FA were involved in performing experiments.

ACKNOWLEDGMENTS

We thank Anne-Marie Girard for technical assistance, Prof. Libo Shan (Texas A&M) for providing several plasmid constructs for sub-cloning. This research was supported by Oregon State University.

SUPPLEMENTARY MATERIAL

The Supplementary Material for this article can be found online at: https://www.frontiersin.org/articles/10.3389/fpls.2019.00635/full#supplementary-material

Supplementary Table S1 | Amino acid sequences and other details of protein fusions used in this study.

Supplementary Table S2 | Primers designed and used for vector constructions.

Supplementary Movie S1 | Dynamics of ER networks labeled by SP-tagRFP-HDEL.

Supplementary Movie S2 | Dynamics of heterogeneous patterns produced by FLS-StRem1.3 BiFC complexes.

Supplementary Figure S1 | Efficient spontaneous reassembly of the two fragments of Venus into BiFC complexes with membrane proteins in *N. benthamiana* leaf cortical cells. **(A)** PM-localized FLS2 and StRem1.3 BiFC complexes formed with free Venus fragments. **(B)** Distribution of BiFC complexes produced by FLS2-VenusN co-expressed with StRem1.3*. **(C)** FLS2, StRem1.3, and its PM-targeting mutant StRem1.3* individually fused with full-length YFP. Scale bars represent 10 μm.

Supplementary Figure S2 | Heterogeneous distribution patterns observed for BiFC complexes produced in *N. benthamiana* leaf cortical cells or *Arabidopsis* mesophyll protoplasts. **(A)** PM-localized FLS2 and StRem1.3 BiFC complexes formed with free YFP fragments. Co-expression of FLS2-YFPn and YFPc-StRem1.3 produced a heterogeneous distribution of the BiFC signal similar to that for Venus BiFC shown in **Figure 1**. **(B)** Transiently expressed in *Arabidopsis* mesophyll protoplasts, FLS2-StRem1.3 BiFC complexes exhibited heterogeneous discrete patches, different from either plasma membrane-localized FLS2-YFP or YFP-StRem1.3, or cytoplasm-localized YFP. Red fluorescence represents chloroplast autofluorescence. BF, bright field. Scale bars in **(A,B)** represent 10 μm.

Supplementary Figure S3 | Orthogonal imaging of SYT1 and FLS2-StRem1.3 BiFC complexes in *N. benthamiana* leaf cortical cells, relative to AtFlotillin1 and FM4-64. **(A)** The *Arabidopsis* tethering protein SYT1 tightly associates with the plasma membrane visualized by FM4-64. **(B)** Regions of the plasma membrane associated with SYT1 show reduced presence of membrane protein AtFlotillin1 fused to tagRFP. **(C)** FLS2-StRem1.3 BiFC complexes tightly associate with the plasma membrane, visualized by FM4-64. **(D)** Regions of the plasma membrane associated with FLS2-StRem1.3 BiFC complexes show reduced presence of AtFlotillin1-tagRFP. **(E)** Subcellular localization of AtFlotillin-1-tagRFP when expressed alone. Scale bars represent 10 μm.

Supplementary Figure S4 | Distribution and kymograph analysis of SYT1, SYT1n, and SYT1-StRem1.3 BiFC complexes co-expressed with ER marker SP-tagRFP-HDEL in *N. benthamiana* leaf cortical cells. **(A)** SYT1-YFP co-expressed with SP-tagRFP-HDEL. Arrowheads highlight bright puncta resembling ER-PM contact sites that stabilize the dynamic ER. **(B)** SYT1n-YFP co-expressed with SP-tagRFP-HDEL, showing coordinated dynamic mobility. **(C)** FLS2-StRem1.3 BiFC complexes co-expressed with SP-tagRFP-HDEL, showing stabilization of dynamic mobility. Kymographs produced as in **Figure 2**. Scale bars represent 10 μm.

Supplementary Figure S5 | Effect of expression time on the distribution of fluorescently tagged full length SYT1, C-terminal C2AC2B domain of SYT1, N-terminal transmembrane domain SYT1n, and BiFC complexes SYT1n&SYT1-C2AC2B, and SYT1n&StRem1.3 in *N. benthamiana* leaf cortical cells. Hpi = hours since *Agrobacterium* infiltration. Scale bars in black color represent 50 μm, and the white scale bars represent 20 μm.

Supplementary Figure S6 | Co-expression of peripheral membrane proteins and SYTn in BiFC complexes in *N. benthamiana* leaf cortical cells results in ER-PM tethering. **(A)** Distribution of peripheral membrane proteins BIK1, PBS1, and CPK21 fused with YFP. **(B)** Distribution and kymograph analysis of BiFC complexes produced by SYT1n-VenusC co-expressed with BIK1-VenusN, PBS1-VenusN, or CPK21-VenusN. **(C)** Puncta observed in BiFC complexes produced by BIK1 & SYT1n, PBS1 & SYT1n, and CPK21 & SYT1n co-localized with wild type SYT1-tagRFP. Kymographs produced as in **Figure 2**. Scale bars represent 10 μm.

Supplementary Figure S7 | Membrane distributions of integral membrane proteins fused to YFP and transiently expressed in *N. benthamiana* leaf cortical cells. **(A)** Subcellular localization of PM IMPs with a cleavable N-terminal signal peptide and single-pass TMD. **(B)** Subcellular localization of tail-anchored SNARE proteins. Qa-SNARE SYP21 and R-SNARE VAMP727 are localized to endosomal vesicles; Qb-SNARE VTI11 and Qc-SNARE SYP61 are localized to the Golgi. **(C)** Subcellular localization of IMPs with multi-pass TMDs. AtDMP1 and AtTPK1 are localized to the vacuolar membrane (tonoplast); SLAH3 is localized on the PM; PIP1 is localized on endosomal membranes. Scale bars in highlighted box represent 5 μm, and all others represent 10 μm.

Supplementary Figure S8 | Effect of expression time on the distribution of BiFC complexes FLS2-VenusN + VenusC-StRem1.3, VenusN-SYP21 + VenusC-StRem1.3, and DMP1-VenusN + VenusC-StRem1.3 in *N. benthamiana* leaf cortical cells. Scale bars in black color represent 50 μm, and the white scale bars represent 20 μm. Hpi = hours since *Agrobacterium* infiltration.

Supplementary Figure S9 | Co-expression of peripheral membrane proteins and StRem1.3 in *N. benthamiana* leaf cortical cells does not result in ER-PM tethering by BiFC complexes. **(A)** Homogenously distributed fluorescent signal observed in BiFC complexes produced by BIK1 & StRem1.3, PBS1 & StRem1.3, CPK21 & StRem1.3, and SNAP33 & StRem1.3. **(B)** The subcellular localization of Qbc-SNARE protein SNAP33 that lacks a TMD. Scale bars represent 10 μm.

Supplementary Figure S10 | Co-expression of PtdIns(3)P binding proteins with the SYT1 N-terminal domain in BiFC complexes in *N. benthamiana* leaf cortical cells does not result in ER-PM tethering. Hrs-2xFYVE, and Vam7-PX proteins are PtdIns(3)P binding proteins while Hrs-2xFYVE* and Vam7-PX* are PtdIns(3)P-non-binding mutants. Kymographs produced as in **Figure 2**. Scale bars represent 10 μm.

REFERENCES

Arrighi, J. F., Barre, A., Ben Amor, B., Bersoult, A., Soriano, L. C., Mirabella, R., et al. (2006). The *Medicago truncatula* lysine motif-receptor-like kinase gene family includes *NFP* and new nodule-expressed genes. *Plant Physiol.* 142, 265–279. doi: 10.1104/pp.106.084657

Asai, S., Ichikawa, T., Nomura, H., Kobayashi, M., Kamiyoshihara, Y., Mori, H., et al. (2013). The variable domain of a plant calcium-dependent protein kinase (CDPK) confers subcellular localization and substrate recognition for NADPH oxidase. *J. Biol. Chem.* 288, 14332–14340. doi: 10.1074/jbc.M112.448910

Bemis, S. M., Lee, J. S., Shpak, E. D., and Torii, K. U. (2013). Regulation of floral patterning and organ identity by *Arabidopsis* ERECTA-family receptor kinase genes. *J. Exp. Bot.* 64, 5323–5333. doi: 10.1093/jxb/ert270

Bockler, S., and Westermann, B. (2014). Mitochondrial ER contacts are crucial for mitophagy in yeast. *Dev. Cell* 28, 450–458. doi: 10.1016/j.devcel.2014.01.012

Borner, G. H. H., Sherrier, D. J., Weimar, T., Michaelson, L. V., Hawkins, N. D., MacAskill, A., et al. (2005). Analysis of detergent-resistant membranes in *Arabidopsis*. Evidence for plasma membrane lipid rafts. *Plant Physiol.* 137, 104–116. doi: 10.1104/pp.104.053041

Boruc, J., Van den Daele, H., Hollunder, J., Rombauts, S., Mylle, E., Hilson, P., et al. (2010). Functional modules in the *Arabidopsis* core cell cycle binary protein–protein interaction network. *Plant Cell* 22, 1264–1280. doi: 10.1105/tpc.109.073635

Bozkurt, T. O., Belhaj, K., Dagdas, Y. F., Chaparro-Garcia, A., Wu, C.-H., Cano, L. M., et al. (2015). Rerouting of plant late endocytic trafficking toward a pathogen interface. *Traffic* 16, 204–226. doi: 10.1111/tra.12245

Bücherl, C. A., Jarsch, I. K., Schudoma, C., Segonzac, C., Mbengue, M., Robatzek, S., et al. (2017). Plant immune and growth receptors share common signalling components but localise to distinct plasma membrane nanodomains. *eLife* 6:e25114. doi: 10.7554/eLife.25114

Burgoyne, T., Patel, S., and Eden, E. R. (2015). Calcium signaling at ER membrane contact sites. *Biochim. Biophys. Acta Mol. Cell Res.* 1853, 2012–2017. doi: 10.1016/j.bbamcr.2015.01.022

Carrasco, S., and Meyer, T. (2011). STIM proteins and the endoplasmic reticulum-plasma membrane junctions. *Annu. Rev. Biochem.* 80, 973–1000. doi: 10.1146/annurev-biochem-061609-165311

Chang, C. L., Hsieh, T. S., Yang, T. T., Rothberg, Karen, G., Azizoglu, D. B., Volk, E., et al. (2013). Feedback regulation of receptor-induced Ca2+ signaling mediated by E-Syt1 and Nir2 at endoplasmic reticulum-plasma membrane junctions. *Cell Rep.* 5, 813–825. doi: 10.1016/j.celrep.2013.09.038

Cheever, M. L., Sato, T. K., de Beer, T., Kutateladze, T. G., Emr, S. D., and Overduin, M. (2001). Phox domain interaction with PtdIns(3)P targets the Vam7 t-SNARE to vacuole membranes. *Nat. Cell Biol.* 3, 613–618. doi: 10.1038/35083000

Delage, E., Ruelland, E., Guillas, I., Zachowski, A., and Puyaubert, J. (2012). Arabidopsis type-III phosphatidylinositol 4-kinases β1 and β2 are upstream of the phospholipase C pathway triggered by cold exposure. *Plant Cell Physiol.* 53, 565–576. doi: 10.1093/pcp/pcs011

Demir, F., Horntrich, C., Blachutzik, J. O., Scherzer, S., Reinders, Y., Kierszniowska, S., et al. (2013). Arabidopsis nanodomain-delimited ABA signaling pathway regulates the anion channel SLAH3. *Proc. Natl. Acad. Sci.* 110, 8296–8301. doi: 10.1073/pnas.1211667110

Dou, D., Kale, S. D., Wang, X., Jiang, R. H., Bruce, N. A., Arredondo, F. D., et al. (2008). RXLR-mediated entry of *Phytophthora sojae* effector Avr1b into soybean cells does not require pathogen-encoded machinery. *Plant Cell* 20, 1930–1947. doi: 10.1105/tpc.107.056093

Dowler, S., Currie, R. A., Campbell, D. G., Deak, M., Kular, G., Downes, C. P., et al. (2000). Identification of pleckstrin-homology-domain-containing proteins with novel phosphoinositide-binding specificities. *Biochem. J.* 351, 19–31. doi: 10.1042/bj3510019

Ebine, K., Okatani, Y., Uemura, T., Goh, T., Shoda, K., Niihama, M., et al. (2008). A SNARE complex unique to seed plants is required for protein storage vacuole biogenesis and seed development of *Arabidopsis thaliana*. *Plant Cell* 20, 3006–3021. doi: 10.1105/tpc.107.057711

Foresti, O., daSilva, L. L. P., and Denecke, J. (2006). Overexpression of the *Arabidopsis* syntaxin PEP12/SYP21 inhibits transport from the prevacuolar compartment to the lytic vacuole *in vivo*. *Plant Cell* 18, 2275–2293. doi: 10.1105/tpc.105.040279

Goder, V., and Spiess, M. (2001). Topogenesis of membrane proteins: determinants and dynamics. *FEBS Lett.* 504, 87–93. doi: 10.1016/S0014-5793(01)02712-0

Gómez-Gómez, L., and Boller, T. (2000). FLS2: an LRR receptor–like kinase involved in the perception of the bacterial elicitor flagellin in *Arabidopsis*. *Mol. Cell* 5, 1003–1011. doi: 10.1016/S1097-2765(00)80265-8

Gookin, T. E., and Assmann, S. M. (2014). Significant reduction of BiFC non-specific assembly facilitates in planta assessment of heterotrimeric G-protein interactors. *Plant J.* 80, 553–567. doi: 10.1111/tpj.12639

Günl, M., Neumetzler, L., Kraemer, F., de Souza, A., Schultink, A., Pena, M., et al. (2011). AXY8 encodes an α-fucosidase, underscoring the importance of apoplastic metabolism on the fine structure of *arabidopsis* cell wall polysaccharides. *Plant Cell* 23, 4025–4040. doi: 10.1105/tpc.111.089193

Guntas, G., Hallett, R. A., Zimmerman, S. P., Williams, T., Yumerefendi, H., Bear, J. E., et al. (2015). Engineering an improved light-induced dimer (iLID) for controlling the localization and activity of signaling proteins. *Proc. Natl. Acad. Sci. U.S.A.* 112, 112–117. doi: 10.1073/pnas.1417910112

Hachez, C., Laloux, T., Reinhardt, H., Cavez, D., Degand, H., Grefen, C., et al. (2014). *Arabidopsis* SNAREs SYP61 and SYP121 coordinate the trafficking of plasma membrane aquaporin PIP2;7 to modulate the cell membrane water permeability. *Plant Cell* 26, 3132–3147. doi: 10.1105/tpc.114.127159

Hammond, G. R. V., Fischer, M. J., Anderson, K. E., Holdich, J., Koteci, A., Balla, T., et al. (2012). PI4P and PI(4,5)P2 are essential but independent lipid determinants of membrane identity. *Science* 337, 727–730. doi: 10.1126/science.1222483

He, J., Scott, J. L., Heroux, A., Roy, S., Lenoir, M., Overduin, M., et al. (2011). Molecular basis of phosphatidylinositol 4-phosphate and ARF1 GTPase recognition by the FAPP1 pleckstrin homology (PH) domain. *J. Biol. Chem.* 286, 18650–18657. doi: 10.1074/jbc.M111.233015

He, Y., Zhou, J., Shan, L., and Meng, X. (2018). Plant cell surface receptor-mediated signaling - a common theme amid diversity. *J. Cell Sci.* 131:jcs209353. doi: 10.1242/jcs.209353

Heese, A., Hann, D. R., Gimenez-Ibanez, S., Jones, A. M. E., He, K., Li, J., et al. (2007). The receptor-like kinase SERK3/BAK1 is a central regulator of innate immunity in plants. *Proc. Natl. Acad. Sci. U.S.A.* 104, 12217–12222. doi: 10.1073/pnas.0705306104

Hegde, R. S., and Keenan, R. J. (2011). Tail-anchored membrane protein insertion into the endoplasmic reticulum. *Nat. Rev. Mol. Cell Biol.* 12, 787–798. doi: 10.1038/nrm3226

Helle, S. C. J., Kanfer, G., Kolar, K., Lang, A., Michel, A. H., and Kornmann, B. (2013). Organization and function of membrane contact sites. *Biochim. Biophys. Acta Mol. Cell Res.* 1833, 2526–2541. doi: 10.1016/j.bbamcr.2013.01.028

Henne, W. M., Liou, J., and Emr, S. D. (2015). Molecular mechanisms of inter-organelle ER–PM contact sites. *Curr. Opin. Cell Biol.* 35, 123–130. doi: 10.1016/j.ceb.2015.05.001

Jahn, R., and Scheller, R. H. (2006). SNAREs — engines for membrane fusion. *Nat. Rev. Mol. Cell Biol.* 7, 631–643. doi: 10.1038/nrm2002

Jarsch, I. K., Konrad, S. S. A., Stratil, T. F., Urbanus, S. L., Szymanski, W., Braun, P., et al. (2014). Plasma membranes are subcompartmentalized into a plethora of coexisting and diverse microdomains in *Arabidopsis* and *Nicotiana benthamiana*. *Plant Cell* 26, 1698–1711. doi: 10.1105/tpc.114.124446

Kale, S. D., Gu, B., Capelluto, D. G., Dou, D., Feldman, E., Rumore, A., et al. (2010). External lipid PI3P mediates entry of eukaryotic pathogen effectors into plant and animal host cells. *Cell* 142, 284–295. doi: 10.1016/j.cell.2010.06.008

Karginov, A. V., Zou, Y., Shirvanyants, D., Kota, P., Dokholyan, N. V., Young, D. D., et al. (2011). Light regulation of protein dimerization and kinase activity in living cells using photocaged rapamycin and engineered FKBP. *J. Am. Chem. Soc.* 133, 420–423. doi: 10.1021/ja109630v

Kargul, J., Gansel, X., Tyrrell, M., Sticher, L., and Blatt, M. R. (2001). Protein-binding partners of the tobacco syntaxin NtSyr1. *FEBS Lett.* 508, 253–258. doi: 10.1016/S0014-5793(01)03089-7

Kasaras, A., and Kunze, R. (2017). Dual-targeting of *Arabidopsis* DMP1 isoforms to the tonoplast and the plasma membrane. *PLoS One* 12:e0174062. doi: 10.1371/journal.pone.0174062

Kasaras, A., Melzer, M., and Kunze, R. (2012). *Arabidopsis* senescence-associated protein DMP1 is involved in membrane remodeling of the ER and tonoplast. *BMC Plant Biol.* 12:54. doi: 10.1186/1471-2229-12-54

Kerppola, T. K. (2006). Design and implementation of bimolecular fluorescence complementation (BiFC) assays for the visualization of protein interactions in living cells. *Nat. Protoc.* 1, 1278–1286. doi: 10.1038/nprot.2006.201

Kerppola, T. K. (2008). Bimolecular fluorescence complementation (BiFC) analysis as a probe of protein interactions in living cells. *Annu. Rev. Biophys.* 37, 465–487. doi: 10.1146/annurev.biophys.37.032807.125842

Kodama, Y., and Hu, C.-D. (2012). Bimolecular fluorescence complementation (BiFC): a 5-year update and future perspectives. *BioTechniques* 53, 285–298. doi: 10.2144/000113943

Kodama, Y., and Hu, C. D. (2010). An improved bimolecular fluorescence complementation assay with a high signal-to-noise ratio. *BioTechniques* 49, 793–805. doi: 10.2144/000113519

Kornmann, B., Currie, E., Collins, S. R., Schuldiner, M., Nunnari, J., Weissman, J. S., et al. (2009). An ER-mitochondria tethering complex revealed by a synthetic biology screen. *Science* 325, 477–481. doi: 10.1126/science.1175088

Krogh, A., Larsson, B., von Heijne, G., and Sonnhammer, E. L. L. (2001). Predicting transmembrane protein topology with a hidden markov model: application to complete genomes. *J. Mol. Biol.* 305, 567–580. doi: 10.1006/jmbi.2000.4315

Kusumi, A., Fujiwara, T. K., Chadda, R., Xie, M., Tsunoyama, T. A., Kalay, Z., et al. (2012). Dynamic organizing principles of the plasma membrane that regulate signal transduction: commemorating the fortieth anniversary of Singer and Nicolson's fluid-mosaic model. *Annu. Rev. Cell Dev. Biol.* 28, 215–250. doi: 10.1146/annurev-cellbio-100809-151736

Kusumi, A., Suzuki, K. G. N., Kasai, R. S., Ritchie, K., and Fujiwara, T. K. (2011). Hierarchical mesoscale domain organization of the plasma membrane. *Trends Biochem. Sci.* 36, 604–615. doi: 10.1016/j.tibs.2011.08.001

Kutateladze, T., and Overduin, M. (2001). Structural mechanism of endosome docking by the FYVE domain. *Science* 291, 1793–1796. doi: 10.1126/science.291.5509.1793

Lee, E., Vanneste, S., Perez-Sancho, J., Benitez-Fuente, F., Strelau, M., Macho, A. P., et al. (2019). Ionic stress enhances ER-PM connectivity via phosphoinositide-associated SYT1 contact site expansion in *Arabidopsis*. *Proc. Natl. Acad. Sci. U.S.A.* 116, 1420–1429. doi: 10.1073/pnas.1818099116

Lee, S. A., Kovacs, J., Stahelin, R. V., Cheever, M. L., Overduin, M., Setty, T. G., et al. (2006). Molecular mechanism of membrane docking by the Vam7p PX domain. *J. Biol. Chem.* 281, 37091–37101. doi: 10.1074/jbc.M608610200

Lefebvre, B., Timmers, T., Mbengue, M., Moreau, S., Hervé, C., Tóth, K., et al. (2010). A remorin protein interacts with symbiotic receptors and regulates bacterial infection. *Proc. Natl. Acad. Sci. U.S.A.* 107, 2343–2348. doi: 10.1073/pnas.0913320107

Lemmon, M. A. (2008). Membrane recognition by phospholipid-binding domains. *Nat. Rev. Mol. Cell Biol.* 9, 99–111. doi: 10.1038/nrm2328

Levy, A., Zheng, J. Y., and Lazarowitz, S. G. (2015). Synaptotagmin SYTA forms ER-plasma membrane junctions that are recruited to plasmodesmata for plant virus movement. *Curr. Biol.* 25, 2018–2025. doi: 10.1016/j.cub.2015.06.015

Lillemeier, B. F., and Klammt, C. (2012). How membrane structures control T cell signaling. *Front. Immunol.* 3:291. doi: 10.3389/fimmu.2012.00291

Limpens, E., Mirabella, R., Fedorova, E., Franken, C., Franssen, H., Bisseling, T., et al. (2005). Formation of organelle-like N_2-fixing symbiosomes in legume root nodules is controlled by *DMI2*. *Proc. Natl. Acad. Sci. U.S.A.* 102, 10375–10380. doi: 10.1073/pnas.0504284102

Lu, D., Wu, S., Gao, X., Zhang, Y., Shan, L., and He, P. (2010). A receptor-like cytoplasmic kinase, BIK1, associates with a flagellin receptor complex to initiate plant innate immunity. *Proc. Natl. Acad. Sci. U.S.A.* 107, 496–501. doi: 10.1073/pnas.0909705107

Lu, S., Chen, L., Tao, K., Sun, N., Wu, Y., Lu, X., et al. (2013). Intracellular and extracellular phosphatidylinositol 3-phosphate produced by *Phytophthora* species is important for infection. *Mol. Plant* 6, 1592–1604. doi: 10.1093/mp/sst047

Maîtrejean, M., Wudick, M. M., Voelker, C., Prinsi, B., Mueller-Roeber, B., Czempinski, K., et al. (2011). Assembly and sorting of the tonoplast potassium channel AtTPK1 and its turnover by internalization into the vacuole. *Plant Physiol.* 156, 1783–1796. doi: 10.1104/pp.111.177816

Madsen, E. B., Madsen, L. H., Radutoiu, S., Olbryt, M., Rakwalska, M., Szczyglowski, K., et al. (2003). A receptor kinase gene of the LysM type is involved in legume perception of rhizobial signals. *Nature* 425, 637–640. doi: 10.1038/nature02045

Matsushima, R., Hayashi, Y., Kondo, M., Shimada, T., Nishimura, M., and Hara-Nishimura, I. (2002). An endoplasmic reticulum-derived structure that is induced under stress conditions in *Arabidopsis*. *Plant Physiol.* 130, 1807–1814. doi: 10.1104/pp.009464

McFarlane, H. E., Lee, E. K., Van Bezouwen, L. S., Ross, B., Rosado, A., and Samuels, A. L. (2017). Multiscale structural analysis of plant ER-PM contact sites. *Plant Cell Physiol.* 58, 478–484. doi: 10.1093/pcp/pcw224

Meng, X., Chen, X., Mang, H., Liu, C., Yu, X., Gao, X., et al. (2015). Differential function of *Arabidopsis* SERK family receptor-like kinases in stomatal patterning. *Curr. Biol.* 25, 2361–2372. doi: 10.1016/j.cub.2015.07.068

Miller, K. E., Kim, Y., Huh, W.-K., and Park, H.-O. (2015). Bimolecular fluorescence complementation (BiFC) analysis: advances and recent applications for genome-wide interaction studies. *J. Mol. Biol.* 427, 2039–2055. doi: 10.1016/j.jmb.2015.03.005

Omasits, U., Ahrens, C. H., Müller, S., and Wollscheid, B. (2014). Protter: interactive protein feature visualization and integration with experimental proteomic data. *Bioinformatics* 30, 884–886. doi: 10.1093/bioinformatics/btt607

Pankiv, S., Alemu, E. A., Brech, A., Bruun, J.-A., Lamark, T., Øvervatn, A., et al. (2010). FYCO1 is a Rab7 effector that binds to LC3 and PI3P to mediate microtubule plus end–directed vesicle transport. *J. Cell Biol.* 188, 253–269. doi: 10.1083/jcb.200907015

Perez-Sancho, J., Tilsner, J., Samuels, A. L., Botella, M. A., Bayer, E. M., and Rosado, A. (2016). Stitching organelles: organization and function of specialized membrane contact sites in plants. *Trends Cell Biol.* 26, 705–717. doi: 10.1016/j.tcb.2016.05.007

Pérez-Sancho, J., Vanneste, S., Lee, E., McFarlane, H. E., Esteban del Valle, A., Valpuesta, V., et al. (2015). The *Arabidopsis* synaptotagmin1 is enriched in endoplasmic reticulum-plasma membrane contact sites and confers cellular resistance to mechanical stresses. *Plant Physiol.* 168, 132–143. doi: 10.1104/pp.15.00260

Perraki, A., Cacas, J. L., Crowet, J. M., Lins, L., Castroviejo, M., German-Retana, S., et al. (2012). Plasma membrane localization of *Solanum tuberosum* remorin from group 1, homolog 3 is mediated by conformational changes in a novel C-terminal anchor and required for the restriction of potato virus X movement. *Plant Physiol.* 160, 624–637. doi: 10.1104/pp.112.200519

Poteser, M., Leitinger, G., Pritz, E., Platzer, D., Frischauf, I., Romanin, C., et al. (2016). Live-cell imaging of ER-PM contact architecture by a novel TIRFM approach reveals extension of junctions in response to store-operated Ca2+-entry. *Sci. Rep.* 6:35656. doi: 10.1038/srep35656

Prinz, W. A. (2014). Bridging the gap: Membrane contact sites in signaling, metabolism, and organelle dynamics. *J. Cell Biol.* 205, 759–769. doi: 10.1083/jcb.201401126

Pu, M., Orr, A., Redfield, A. G., and Roberts, M. F. (2010). Defining specific lipid binding sites for a peripheral membrane protein *in situ* using subtesla field-cycling NMR. *J. Biol. Chem.* 285, 26916–26922. doi: 10.1074/jbc.M110.123083

Qi, D., Dubiella, U., Kim, S. H., Sloss, D. I., Dowen, R. H., Dixon, J. E., et al. (2014). Recognition of the protein kinase AVRPPHB SUSCEPTIBLE1 by the Disease Resistance Protein RESISTANCE TO PSEUDOMONAS SYRINGAE5 Is Dependent on S-Acylation and an Exposed Loop in AVRPPHB SUSCEPTIBLE1. *Plant Physiol.* 164, 340–351. doi: 10.1104/pp.113.227686

Radutoiu, S., Madsen, L. H., Madsen, E. B., Felle, H. H., Umehara, Y., Grønlund, M., et al. (2003). Plant recognition of symbiotic bacteria requires two LysM receptor-like kinases. *Nature* 425, 585–592. doi: 10.1038/nature02039

Raffaele, S., Bayer, E., Lafarge, D., Cluzet, S., German Retana, S., Boubekeur, T., et al. (2009). Remorin, a solanaceae protein resident in membrane rafts and plasmodesmata, impairs potato virus X movement. *Plant Cell* 21, 1541–1555. doi: 10.1105/tpc.108.064279

Rapoport, T. A. (2007). Protein translocation across the eukaryotic endoplasmic reticulum and bacterial plasma membranes. *Nature* 450, 663–669. doi: 10.1038/nature06384

Remy, I., and Michnick, S. W. (2004). Regulation of apoptosis by the Ft1 protein, a new modulator of protein kinase B/Akt. *Mol. Cell. Biol.* 24, 1493–1504. doi: 10.1128/MCB.24.4.1493-1504.2004

Resh, M. D. (2013). Covalent lipid modifications of proteins. *Curr. Biol.* 23, R431–R435. doi: 10.1016/j.cub.2013.04.024

Russinova, E., Borst, J. W., Kwaaitaal, M., Cano-Delgado, A., Yin, Y., Chory, J., et al. (2004). Heterodimerization and endocytosis of *Arabidopsis*

brassinosteroid receptors BRI1 and AtSERK3 (BAK1). *Plant Cell* 16, 3216–3229. doi: 10.1105/tpc.104.025387

Saheki, Y., and De Camilli, P. (2017). Endoplasmic reticulum-plasma membrane contact sites. *Annu. Rev. Biochem.* 86, 659–684. doi: 10.1146/annurev-biochem-061516-044932

Saka, Y., Hagemann, A., Piepenburg, O., and Smith, J. C. (2007). Nuclear accumulation of Smad complexes occurs only after the midblastula transition in *Xenopus*. *Development* 134, 4209–4218. doi: 10.1242/dev.010645

Sanmartín, M., Ordóñez, A., Sohn, E. J., Robert, S., Sánchez-Serrano, J. J., Surpin, M. A., et al. (2007). Divergent functions of VTI12 and VTI11 in trafficking to storage and lytic vacuoles in *Arabidopsis*. *Proc. Natl. Acad. Sci. U.S.A.* 104, 3645–3650. doi: 10.1073/pnas.0611147104

Saravanan, R. S., Slabaugh, E., Singh, V. R., Lapidus, L. J., Haas, T., and Brandizzi, F. (2009). The targeting of the oxysterol-binding protein ORP3a to the endoplasmic reticulum relies on the plant VAP33 homolog PVA12. *Plant J.* 58, 817–830. doi: 10.1111/j.1365-313X.2009.03815.x

Schapire, A. L., Voigt, B., Jasik, J., Rosado, A., Lopez-Cobollo, R., Menzel, D., et al. (2008). *Arabidopsis* synaptotagmin 1 is required for the maintenance of plasma membrane integrity and cell viability. *Plant Cell* 20, 3374–3388. doi: 10.1105/tpc.108.063859

Schulz, P., Herde, M., and Romeis, T. (2013). Calcium-dependent protein kinases: hubs in plant stress signaling and development. *Plant Physiol.* 163, 523–530. doi: 10.1104/pp.113.222539

Serna, L. (2005). A simple method for discriminating between cell membrane and cytosolic proteins. *New Phytol.* 165, 947–952. doi: 10.1111/j.1469-8137.2004.01278.x

Shyu, Y. J., Liu, H., Deng, X., and Hu, C. D. (2006). Identification of new fluorescent protein fragments for bimolecular fluorescence complementation analysis under physiological conditions. *BioTechniques* 40, 61–66. doi: 10.2144/000112036

Simon, M. L. A., Platre, M. P., Marquès-Bueno, M. M., Armengot, L., Stanislas, T., Bayle, V., et al. (2016). A PtdIns(4)P-driven electrostatic field controls cell membrane identity and signalling in plants. *Nat. Plants* 2:16089. doi: 10.1038/nplants.2016.89

Smit, P., Limpens, E., Geurts, R., Fedorova, E., Dolgikh, E., Gough, C., et al. (2007). *Medicago* LYK3, an entry receptor in rhizobial nodulation factor signaling. *Plant Physiol.* 145, 183–191. doi: 10.1104/pp.107.100495

Snider, J., Hanif, A., Lee, M. E., Jin, K., Yu, A. R., Graham, C., et al. (2013). Mapping the functional yeast ABC transporter interactome. *Nat. Chem. Biol.* 9, 565–572. doi: 10.1038/nchembio.1293

Speth, E. B., Imboden, L., Hauck, P., and He, S. Y. (2009). Subcellular localization and functional analysis of the *Arabidopsis* GTPase RabE. *Plant Physiol.* 149, 1824–1837. doi: 10.1104/pp.108.132092

Stefano, G., Renna, L., and Brandizzi, F. (2014). The endoplasmic reticulum exerts control over organelle streaming during cell expansion. *J. Cell Sci.* 127, 947–953. doi: 10.1242/jcs.139907

Stefano, G., Renna, L., Wormsbaecher, C., Gamble, J., Zienkiewicz, K., and Brandizzi, F. (2018). Plant endocytosis requires the ER membrane-anchored proteins VAP27-1 and VAP27-3. *Cell Rep.* 23, 2299–2307. doi: 10.1016/j.celrep.2018.04.091

Stillwell, W. (2016). "Chapter 6 - membrane proteins," in *An Introduction to Biological Membranes, 2nd Edn.* (Amsterdam: Elsevier), 89–110. doi: 10.1016/B978-0-444-63772-7.00006-3

Stracke, S., Kistner, C., Yoshida, S., Mulder, L., Sato, S., Kaneko, T., et al. (2002). A plant receptor-like kinase required for both bacterial and fungal symbiosis. *Nature* 417:959. doi: 10.1038/nature00841

Tao, K., Waletich, J. R., Wise, H., Arredondo, F., and Tyler, B. M. (2019). Tethering of multi-vesicular bodies and the tonoplast to the plasma membrane in plants. *Front. Plant Sci.* 10:636. doi: 10.3389/fpls.2019.00636

Tóth, K., Stratil, T. F., Madsen, E. B., Ye, J., Popp, C., Antolín-Llovera, M., et al. (2012). Functional domain analysis of the remorin protein LjSYMREM1 in *Lotus japonicus*. *PLoS ONE* 7:e30817. doi: 10.1371/journal.pone.0030817

Van Leeuwen, W., Vermeer, J. E. M., Gadella, T. W. J., and Munnik, T. (2007). Visualization of phosphatidylinositol 4,5-bisphosphate in the plasma membrane of suspension-cultured tobacco BY-2 cells and whole *Arabidopsis* seedlings. *Plant J.* 52, 1014–1026. doi: 10.1111/j.1365-313X.2007.03292.x

Varshney, P., Yadav, V., and Saini, N. (2016). Lipid rafts in immune signalling: current progress and future perspective. *Immunology* 149, 13–24. doi: 10.1111/imm.12617

Vermeer, J. E., Thole, J. M., Goedhart, J., Nielsen, E., Munnik, T., and Gadella, T. W. Jr. (2009). Imaging phosphatidylinositol 4-phosphate dynamics in living plant cells. *Plant J.* 57, 356–372. doi: 10.1111/j.1365-313X.2008.03679.x

Vermeer, J. E., van Leeuwen, W., Tobena-Santamaria, R., Laxalt, A. M., Jones, D. R., Divecha, N., et al. (2006). Visualization of PtdIns3P dynamics in living plant cells. *Plant J.* 47, 687–700. doi: 10.1111/j.1365-313X.2006.02830.x

Vögler, O., Barceló, J. M., Ribas, C., and Escribá, P. V. (2008). Membrane interactions of G proteins and other related proteins. *Biochim. Biophys. Acta* 1778, 1640–1652. doi: 10.1016/j.bbamem.2008.03.008

Walter, P., and Johnson, A. E. (1994). Signal sequence recognition and protein targeting to the endoplasmic reticulum membrane. *Annu. Rev. Cell Biol.* 10, 87–119. doi: 10.1146/annurev.cb.10.110194.000511

Wang, L., Li, H., Lv, X., Chen, T., Li, R., Xue, Y., et al. (2015). Spatiotemporal dynamics of the BRI1 receptor and its regulation by membrane microdomains in living *Arabidopsis* cells. *Mol. Plant* 8, 1334–1349. doi: 10.1016/j.molp.2015.04.005

Wang, P., Hawes, C., and Hussey, P. J. (2017). Plant endoplasmic reticulum-plasma membrane contact sites. *Trends Plant Sci.* 22, 289–297. doi: 10.1016/j.tplants.2016.11.008

Wang, P., Hawkins, T. J., Richardson, C., Cummins, I., Deeks, M. J., Sparkes, I., et al. (2014). The plant cytoskeleton NET3C and VAP27 mediate the link between the plasma membrane and endoplasmic reticulum. *Curr. Biol.* 24, 1397–1405. doi: 10.1016/j.cub.2014.05.003

Wang, P., Richardson, C., Hawkins, T. J., Sparkes, I., Hawes, C., and Hussey, P. J. (2016). Plant VAP27 proteins: domain characterization, intracellular localization and role in plant development. *New Phytol.* 210, 1311–1326. doi: 10.1111/nph.13857

Wong, K. A., and O'Bryan, J. P. (2011). Bimolecular fluorescence complementation. *J. Vis. Exp.* 50:e2643. doi: 10.3791/2643

Wudick, M. M., Luu, D. T., and Maurel, C. (2009). A look inside: localization patterns and functions of intracellular plant aquaporins. *New Phytol.* 184, 289–302. doi: 10.1111/j.1469-8137.2009.02985.x

Yagisawa, H., Sakuma, K., Paterson, H. F., Cheung, R., Allen, V., Hirata, H., et al. (1998). Replacements of single basic amino acids in the pleckstrin homology domain of phospholipase C-δ1 alter the ligand binding, phospholipase activity, and interaction with the plasma membrane. *J. Biol. Chem.* 273, 417–424. doi: 10.1074/jbc.273.1.417

Yamazaki, T., Takata, N., Uemura, M., and Kawamura, Y. (2010). Arabidopsis synaptotagmin SYT1, a type I signal-anchor protein, requires tandem C2 domains for delivery to the plasma membrane. *J. Biol. Chem.* 285, 23165–23176. doi: 10.1074/jbc.M109.084046

Yoo, S. D., Cho, Y. H., and Sheen, J. (2007). *Arabidopsis* mesophyll protoplasts: a versatile cell system for transient gene expression analysis. *Nat. Protoc.* 2, 1565–1572. doi: 10.1038/nprot.2007.199

Zamyatnin, A. A., Solovyev, A. G., Bozhkov, P. V., Valkonen, J. P. T., Morozov, S. Y., and Savenkov, E. I. (2006). Assessment of the integral membrane protein topology in living cells. *Plant J.* 46, 145–154. doi: 10.1111/j.1365-313X.2006.02674.x

Zipfel, C., Kunze, G., Chinchilla, D., Caniard, A., Jones, J. D. G., Boller, T., et al. (2006). Perception of the bacterial PAMP EF-Tu by the receptor EFR restricts *Agrobacterium*-mediated transformation. *Cell* 125, 749–760. doi: 10.1016/j.cell.2006.03.037

Conflict of Interest Statement: The authors declare that the research was conducted in the absence of any commercial or financial relationships that could be construed as a potential conflict of interest.